

3. MATERIALS PROCESSING TECHNOLOGY

A. Oxidative Stabilization of PAN Fiber Precursor

Principal Investigator: Felix L. Paulauskas

Oak Ridge National Laboratory

Oak Ridge, TN 37831-8048

(865) 576-3785; fax: (865) 574-8257; e-mail: paulauskasfl@ornl.gov

Project Manager, Composites: C. David Warren

Oak Ridge National Laboratory

P.O. Box 2008, Oak Ridge, TN 37831-6065

(865) 574-9693; fax: (865) 576-4963; e-mail: warrencd@ornl.gov

Technology Development Area Specialist: Sidney Diamond

(202) 586-8032; fax (202) 586-2476; e-mail: sid.diamond@hq.doe.gov

Field Technical Manager: Philip S. Sklad

(865) 574-5069; fax:(865) 576-4963; e-mail: skladps@ornl.gov

Participants

Terry L. White and

Kenneth D. Yarborough, Oak Ridge National Laboratory

Professor Joseph Spruiell, University of Tennessee

Daniel Sherman, Atmospheric Glow Technologies

Contractor: Oak Ridge National Laboratory

Contract No.: DE-AC05-00OR22725

Objectives

- Develop an improved technique for oxidizing carbon fiber precursor with increased line speed, reduced carbon fiber cost, and reduced equipment footprint.
- Verify that fiber properties satisfy automotive and heavy vehicle manufacturers' requirements.
- Conduct a preliminary evaluation of the new oxidation technique's cost impact.

Approach

- Investigate plasma processing in an evacuated reactor, with plasma generated remotely and pumped to the fibers (remote exposure).
- Investigate plasma processing in an atmospheric pressure reactor, with fibers located near the plasma generator (direct exposure).
- Conduct parametric studies to correlate processing parameters and fiber properties.
- Characterize fibers to confirm that they satisfy program requirements.

Accomplishments

- Constructed and evaluated multiple reactor designs for both remote and direct plasma exposure strategies.
- Demonstrated partial oxidation using plasma processing.
- Conducted dielectric measurements to determine the acceptable range of a critical processing variable. The results led to significant changes in the reactor design and processing parameters.

Future Direction

- Utilize an evacuated plasma reactor to conduct studies on reactive chemical species optimization.
- Focus on atmospheric plasma processing as the best route to a robust, rapid oxidation technique. Continue refining the reactor design and processing protocols to achieve complete fiber oxidation.
- Conduct parametric studies and fiber characterization to better understand process effects and the processing window and to quantify fiber properties.
- Conduct rate-effect studies and preliminary cost analysis.

Introduction

The purpose of this project is to investigate and develop a plasma processing technique to rapidly and inexpensively oxidize a polyacrylonitrile (PAN) precursor. Oxidative stabilization is a slow thermal process that typically consumes 70% or more of the processing time in a conventional carbon fiber manufacturing line. A rapid oxidation process could dramatically increase the manufacturing line throughput and appreciably lower the fiber cost. A related project has already demonstrated the potential for greatly increasing line speed in the carbonization and graphitization stages, but the oxidation time must be greatly reduced to fully exploit faster carbonization and graphitization. This project intends to develop a plasma oxidation module that integrates with other advanced fiber processing modules to produce inexpensive carbon fiber with properties suitable for use by the automotive industry. Critical technical criteria include (1) 25 Msi tensile modulus, 250 ksi ultimate strength, and 1.0% ultimate strain in the finished fiber; (2) acceptably uniform properties over the length of the fiber tow; (3) repeatable and controllable processing; (4) and significant

unit cost reduction in comparison to conventional processing

Project Deliverable

At the end of this project, complete fiber oxidation will have been demonstrated using a plasma oxidation process. Successful completion of this deliverable is expected to be followed by rate studies and equipment scale-up in a future project.

Technical Approach

Two plasma generation and control techniques are under investigation. The technique called "direct exposure" utilizes non-equilibrium, nonthermal plasma at atmospheric pressure, with the fiber transported through the plasma. The other technique called "remote exposure" uses a more conventional, evacuated (negative pressure) plasma reactor that pumps plasma with the active chemical species from the reactor chamber to another processing chamber in/through which the fibers are transported. Generation and control of chemically reactive species is more readily accomplished in the remote exposure technique. Direct expo-

sure provides better thermal control. Various fiber characterization tools and instruments are used to conduct parametric studies and physical, mechanical, and morphological evaluations of the fibers to optimize the process.

Experimental Results—Remote Exposure

Density measurements and morphological studies were conducted to confirm that the plasma is indeed oxidizing the fiber in remote exposure (evacuated reactor) process-

ing. As oxidation proceeds, the fiber density should increase, with a fully oxidized fiber having specific gravity of ~1.4. Representative density data is tabulated in Table 1, showing that processing is proceeding. In some cases, the density approaches that of fiber exiting the first oxidation furnace in a conventional line. This is remarkable because the plasma oxidation chamber is quite compact, and the experimental work is still in the early feasibility stage.

Table 1. Pycnometer density data

	Pycnometer density, g/cc		Note
Reference values	1.1986		As-received 3K PAN precursor
	1.1485		Unprocessed, after 3.5 h at 0.8 in. Hg vacuum pressure
	1.1428		Unprocessed, after 1.17 h at 0.8 in. Hg vacuum pressure
	~1.25		Exit of 1 st conventional oxidation furnace
	~1.4		Fully oxidized precursor, conventionally processed
Sample ID	Pre-plasma	Post-plasma	
2C	1.1483	1.2267 1.2172	Low pre-plasma density attributed to short preheater that was later lengthened
4C	1.1898	1.2389	
5C	1.1898	1.1996 1.2208 1.2389 1.2398	
6C	1.18 98	1.2821 1.2610	Brown spots on post-plasma fiber
7C	1.18 98	2.2178	
8C	1.18 98	1.2364	
9C		1.2118	
All plasma processing data generated using remote exposure plasma configuration and medium pre-heater temperature profile. Pre-plasma data point is taken after thermal pre-heating and before exposure to plasma.			

X-ray diffraction and dynamic scanning calorimetry (DSC) data were obtained for selected samples that have been partially oxidized by remote exposure to plasma. The DSC data presented were obtained by scanning from 100°C to 350°C at a scanning rate of 5°C per min. This rate was cho-

sen for comparison with data from the literature.

Figure 1(a) compares partially processed plasma precursor to a commercial grade virgin PAN precursor and a fully stabilized sample prepared by the conventional process. This figure illustrates the changes to be

expected in the diffraction patterns during oxidation and those that are occurring with partial plasma oxidation. It can be seen from the X-ray diffraction data in Figure 1(b) that the samples of commercial grade Stage 1-1 through Stage 1-5 and two selected plasma processed samples all exhibit similar diffraction patterns and that they have not changed significantly from the pattern of the PAN precursor. It is therefore difficult to tell how far the Oak Ridge National Laboratory (ORNL) samples have progressed in the oxidation process from

diffraction data alone (i.e., X-ray diffraction analysis is not sensitive enough in the first oxidation stage). Oxidation samples were tested in the DSC to further discriminate the oxidation level achieved. The peak temperature decreases and the exothermic heat of reaction decreases as the precursor is oxidized more. ORNL samples were also tested in the DSC and compared to the commercial grade samples. The plasma-processed sample appears to have been affected by the oxidation process to a degree similar to the commercial grade process.

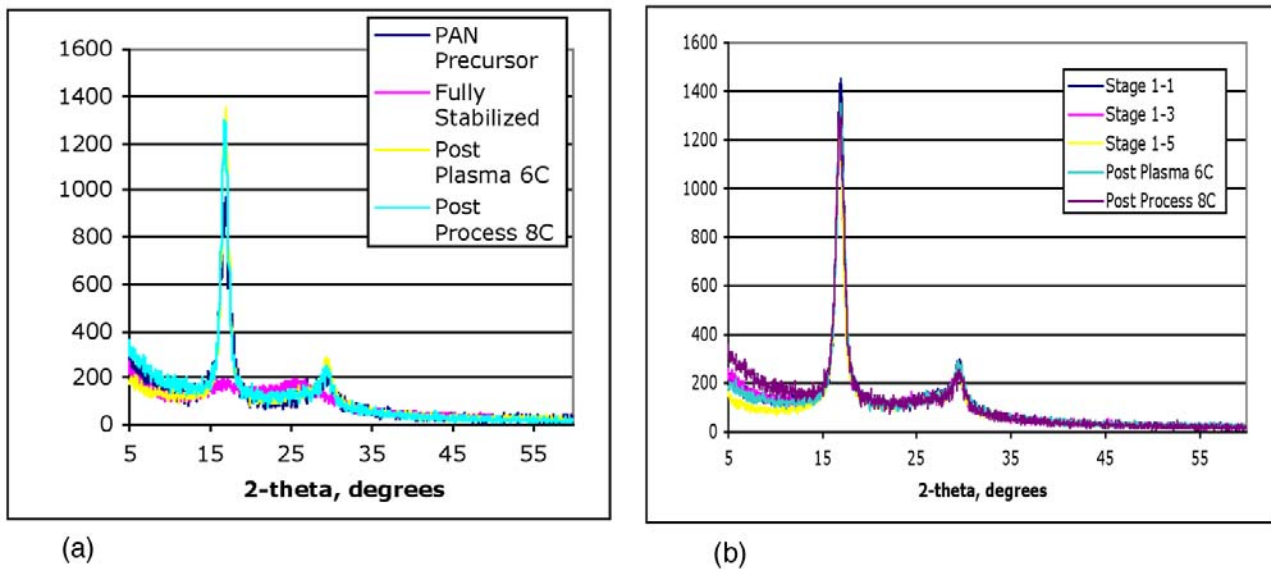


Figure 1. Diffractograms comparing partially plasma-oxidized precursor with virgin precursor and fully stabilized PAN (a). Diffractograms comparing partially plasma-oxidized precursor with partially oxidized precursor taken at various points partway through the first conventional oxidation furnace (b).

Experimental Results—Direct Exposure

Direct exposure in plasma at near atmospheric pressure is expected to provide superior thermal control because the gas flow should convectively heat or cool the fibers. This is deemed particularly important to avoid fiber melting from the exothermic reactions associated with the PAN cross-linking that occurs during stabilization. However, the mean free path of the chemically reactive

species is shorter by orders of magnitude than it is in an evacuated environment, and this makes it very difficult to find a combination of process parameters that will oxidize the fibers with acceptable residence time.

The experimental program was focused principally on direct exposure techniques in the last half of FY 2003. Most of the effort was devoted to designing and testing a number of different reactor configurations. Atmospheric pressure plasma processing is itself

a technology in its infancy, and utilizing it to oxidize fiber is necessarily an intensive trial and error effort. A limited degree of oxidation has been achieved— to 1.25 specific gravity starting with material at 1.21 specific gravity. Oxidation levels as well as residence times and uniformity need to be improved.

Because the interaction of atmospheric pressure plasma with carbon fiber is not yet well understood, it has been very difficult to achieve sustained and stable reactor operation. Nevertheless, several experiments in the September 2003 time frame produced prom-

ising results. One of the major objectives for the first half of FY 2004 will be to select one or more promising reactor configurations and achieve sustained stable operation, with a corresponding increase in the achieved degree of fiber oxidation.

Figure 2 shows several atmospheric pressure reactor designs that were constructed and tested. Each succeeding reactor design included features that were intended to improve the rate or control the oxidation process in comparison to earlier generations.

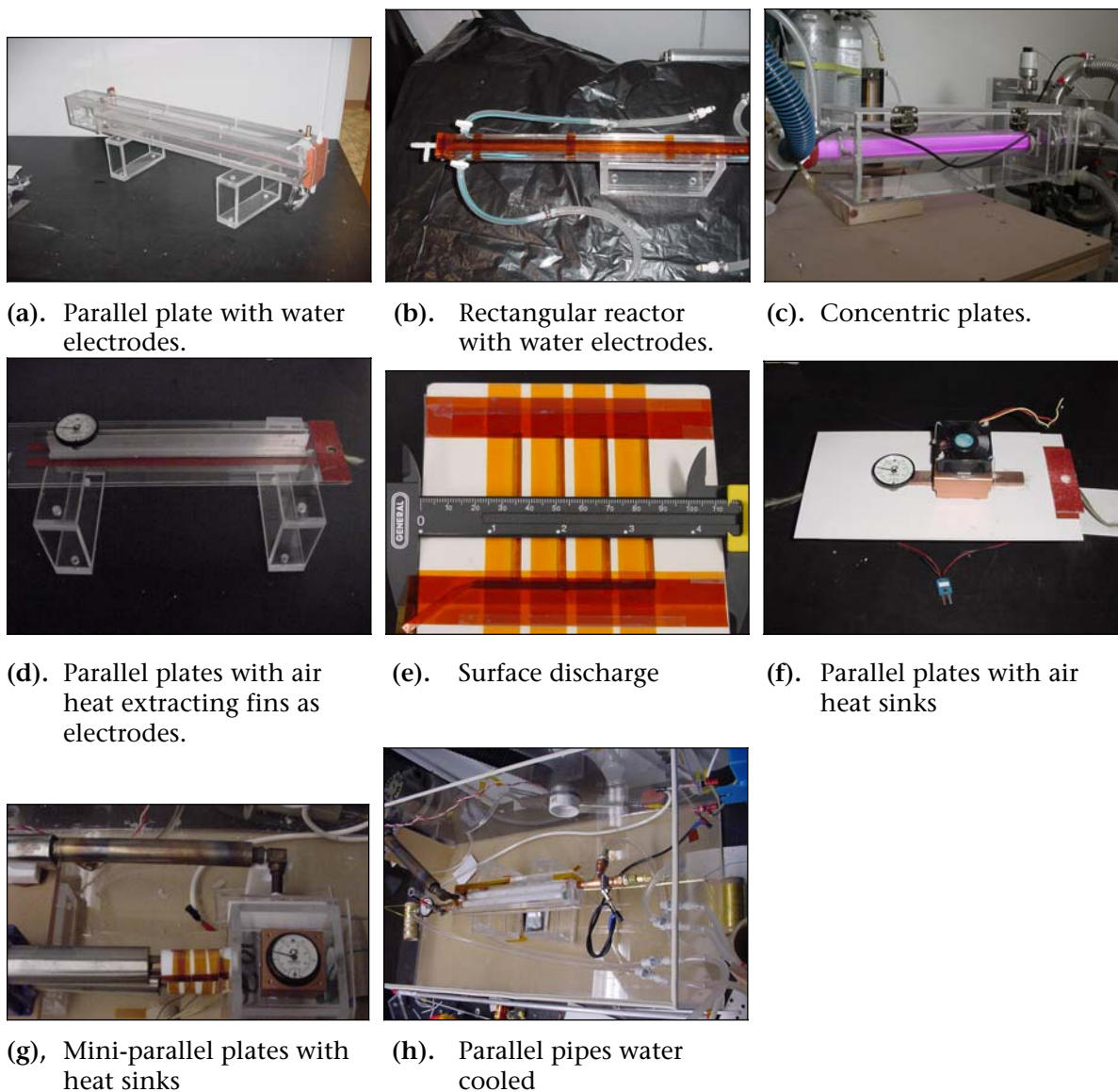


Figure 2. Remote exposure reactors.

Parametric Studies

Techniques and hardware were developed for measuring the fiber dielectric properties over a selected range of oxidation-processing conditions. This is an extension of technology for monitoring the carbonization process by measuring the fiber dielectric properties. Correlation of the dielectric properties with processing conditions is expected to yield insights into the process dynamics. Unoxidized PAN is an insulator, rendering dc conductivity measurements of limited use for monitoring oxidation progress; hence, dielectric monitoring is especially valuable for oxidation. Initial results led to significant changes in the reactor design and processing parameters. This work is continuing, with improvements being made to the dielectric measurement system.

Education

The materials characterization has been conducted in partnership with the University of Tennessee's (UT's) materials science department. Two UT graduate students were engaged to provide characterization support to the project.

Conclusions

The development of plasma-based oxidation technology has progressed at a pace consistent with funding and effort expended. Several generations of hardware have been constructed for experiments in both evacuated reactors and atmospheric pressure reactors. Plasma has been shown to effect partial oxidation of PAN fibers. The researchers expect to achieve complete fiber oxidation in FY 2004.

B. Wrought Magnesium Alloy/Process Development

Principal Investigator: S. R. Agnew
University of Virginia
116 Engineer's Way
PO Box 400745 Charlottesville, VA 22904-4745

Principal Investigator: J. A. Horton
Oak Ridge National Laboratory
P.O. Box 2008, Oak Ridge, TN 37831-6115
(865)74-5575; fax: (865) 574-825; hortonja@ornl.gov

Technology Development Area Specialist: Sidney Diamond
(202) 586-8032; fax: (202) 586-1600; e-mail: sid.diamond@ee.doe.gov
Field Technical Manager: Philip S. Sklad
(865) 574-5069; fax: (865) 576-4963; e-mail: skladps@ornl.gov

Contractor: Oak Ridge National Laboratory
Contract No.: DE-AC05-00OR22725

Objectives

- Develop wrought magnesium alloys with better formability than current magnesium alloys.
- Investigate new processing techniques for cost control, texture control, and formability.
- Contribute to basic understanding of deformation, processing, and alloy behavior for this lightweight metal.

Approach

- Explore new processing schemes for magnesium alloy sheets.
- Evaluate the practical formability (deep drawability) of new alloys.
- Determine deformation mechanisms using experimentation and simulation.

Accomplishments

- Demonstrated feasibility of utilizing infrared heating for sheet processing.
- Used equal channel angular extrusion to show the potent effect of crystallographic texture on mechanical behavior.
- Determined that the hardening response, which is critical for secondary forming operations, could be improved by combining low-temperature twinning deformation and annealing or high temperature deformation.
- Demonstrated that initial bending and unbending trials did not change the texture and mechanical behavior as expected from old anecdotal reports.

- Demonstrated that an alloy with a high r-value performed better than the industry standard AZ31 through use of the deep drawing tests of our experimental ductile alloys.
- Demonstrated that polycrystal plasticity simulation provides an explanation for changes in r-value and formability with loading orientation and temperature in terms of the fundamental deformation mechanisms of magnesium (i.e., slip of basal and nonbasal dislocations.)

Future Direction

- Conduct a pilot-plant scale test of infrared processing of wrought magnesium sheet fabrication.
- Pursue combinations of annealing and bending of sheet alloys for texture and property control.
- Define further correlations of r-values and refine more new alloys for better formability.
- Develop a warm formability test more relevant to industrial practice (plane strain.)

Introduction

The world market for magnesium has changed substantially in the last couple years. The emergence of China as the leading producer (~50% of the market) of inexpensive magnesium alloys has led to circumstances where magnesium alloy die cast or thixomoulded parts can be less expensive, in some instances, than their aluminum alloy counterparts. There are pros and cons to these events. On the one hand, it may make magnesium a more attractive material choice for a number of applications, such as the chassis of laptop computers. On the other hand there are concerns that the Chinese producers may drive western competitors out of business. Additionally, the reason the prices are so low is that these new producers do not have to abide by western standards of environmental protection and energy conservation. Thus, the end goal of magnesium usage for transportation (energy savings and reduction of emissions) may be lost in a life-cycle analysis which includes production. It is still unclear what the final outcome will be.

In the case of wrought magnesium, the situation is less clear. German steel makers (Thyssen Krupp and Salzgitter) have new magnesium rolling facilities that represent millions of dollars of capital investment. Another leading steel producer from Korea,

POSCO, is making plans to enter the magnesium sheet market as well. Here in the United States, the formerly lone magnesium sheet producer in the world, Spectrulite, was in bankruptcy throughout the past year. However, the assets for casting and sheet production were just purchased by Magnesium Elektron (MEL), of the United Kingdom. MEL has been an innovative leader in magnesium technology (particularly gravity-cast alloy development). An example is the WE class of alloys they have developed during the past 20 years, which is eagerly consumed by the Formula One race car industry for engine parts and is considered for some helicopter transmission applications.

Magnesium sheet manufacturers must face a number of technical issues, including

- Rolling magnesium into thin gage sheet currently leads to expensive solutions.
- Obtaining an excellent surface finish has been difficult.
- Corrosion performance of wrought alloys has lagged that of die-cast alloys.
- Sheet formability is limited at room temperature.

Our work during FY 2003 focused on sheet formability issues, and we began

addressing the concerns associated with the cost of sheet products.

It is recognized that two issues limit the sheet formability of magnesium alloys at low temperatures. First, the hexagonal close-packed structure and the apparent lack of easy deformation mechanisms do not accommodate arbitrary strain paths. Second, magnesium alloys develop strong crystallographic texture during wrought processing. We have investigated three possible thermomechanical processing routes to alter the strong crystallographic texture.

- upset forging of conventional extrusions (during FY 2002)
- equal channel angular extrusion (ECAE)
- bending-unbending of conventional sheets.

Texture Control and Hardening Response

ECAE was successful in altering the texture significantly. In fact, the new texture was completely distinct from the conventional extrusion texture; however, it was surprisingly stronger than the conventional extrusion texture (Figure 1). Tensile test results emphasize how potent an effect texture has on the behavior of magnesium (Figure 2). For an alloy that normally only has 15–20% ductility in the extruded condition, we achieved an elongation of >40% along the extrusion axis [see also T. Mukai, M. Yamanoi, H. Watanabe and K. Higashi, *Scripta mater.* **45** (2001) 89 and W. J. Kim, C. W. An, Y. S. Kim and S. I. Hong *Scripta Mater.* **47** (2002) 39]. Furthermore, one of the frequently cited liabilities of magnesium extrusions was also overcome; there is no apparent tension/compression asymmetry. Namely, the flow curves in tension and compression along the extrusion axis look essentially the same. If this process could be altered to produce sheet material, there may be some opportunities to produce sheets with remarkably distinct textures from conventional processes.

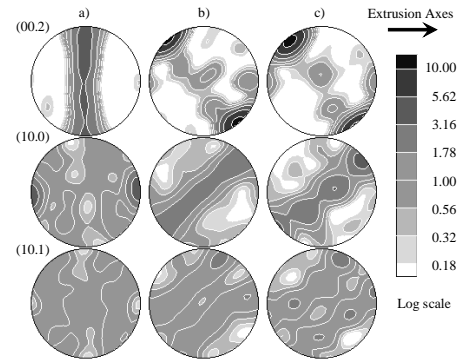


Figure 1. Pole figures (equal area projection) measured using neutron diffraction at Los Alamos National Laboratory show the crystallographic textures in (a) conventionally extruded, (b) ECA processed, and (c) annealed AZ31B. Note stronger texture in the ECA processed materials.

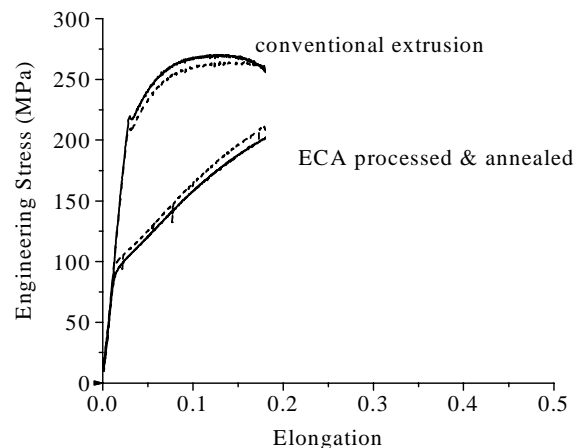


Figure 2. Tensile test results from conventionally extruded and ECA processed and annealed material. The ECA material shows an impressive ductility improvement. The load drops in the flow curve suggest some twinning activity. Curves from two samples of each type demonstrate the reproducibility of the results.

In FY 2002, we explored upset forging of conventional extrusions because the two major deformation mechanisms in magnesium (basal slip and mechanical twinning) would lead to rapid texture

evolution under these conditions. The texture-altered material could then be used to test how the materials mechanical behavior would change. First, the material was compression tested over a range of temperatures, to identify the temperature regime where twinning dominates (since twinning gives rise to a characteristic flow curve in textured magnesium as shown in Figure 3.) Then processing routes involving primarily twinning (at low temperature) and

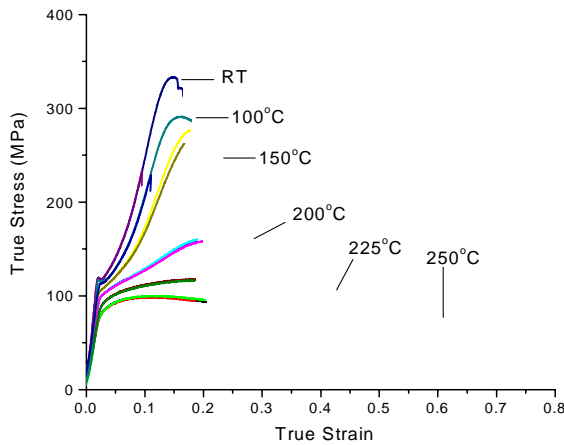


Figure 3. Stress-strain curves from compression tests along the extrusion axis have a shape characteristic of deformation twinning at low temperatures and that of dynamic recrystallization at higher temperatures.

slip (at high temperature) were used to alter the texture. Finally, the material was annealed in order to eliminate the deleterious effect of prior deformation on ductility. The test results suggest that even though the overall ductility was limited to about 30%, it is possible to strongly change the hardening response, which is critical for secondary forming operations (Figure 4). One of the reasons that magnesium alloys fail to exhibit excellent sheet formability is their lack of strain hardening. Altering the texture is, thus, shown to be potent means of altering this trend.

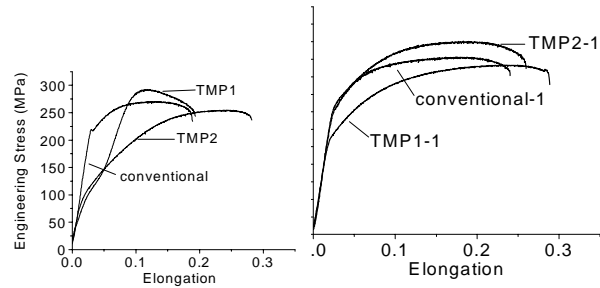


Figure 4. Tensile tests (a) results from conventionally extruded, room temperature upset (TMP1) and high temperature upset (TMP2) and (b) results from the same material after annealing.

Bending-Unbending

During FY 2003, bending-unbending procedure was explored on the basis of some anecdotal reports from some old texts that stated that magnesium’s ductility was improved by passing it repeatedly through “sheet levelers,” which force the sheet to bend and unbend. The supposed reason for this behavior is very similar to the logic described above for the upsetting of extrusions. The material on the inner side of the bend is forced into compression within the plane of the sheet. This results in extensive twinning of the material on the inner side of the bent sheet. Further, the texture is strongly altered by the presence of twins (Figure 5). Unfortunately, we found that the unbending resulted in “untwining” as well. Thus, the resulting texture alteration after bending and unbending is not significant. Similarly, the change in the mechanical behavior is not significant (Figure 6). It is suggested that suitable combinations of annealing and bending may result in a benefit to the formability of magnesium sheets, so this will continue to be an area of active research in FY 2004.

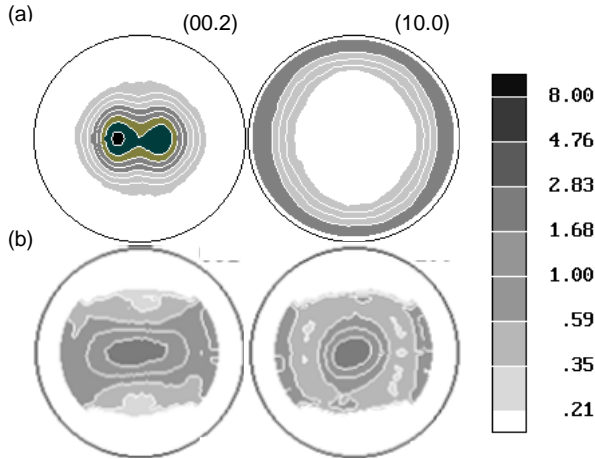


Figure 5. X-ray pole figures show (a) strong initial rolling texture and (b) the texture in a bent sheet that is strongly altered from the initial condition.

Infrared Lamp Sheet Processing

More recently, we have been exploring the possibility of economizing the magnesium alloy sheet fabrication process. The main problem is that magnesium must be rolled at a slightly elevated temperature and that the rolls will quickly extract all of the heat from thin-gage sheets. In current industrial practice, the final “cold” rolling is performed one or two rolling passes at a time with intermediate recovery anneals and reheats. This is very inefficient and drives the cost of inexpensive raw material to a very high price for the final wrought product.

Using rapid radiant heating, it is suggested that magnesium could be efficiently warm rolled. The material could be passed through a radiant furnace between rolling reductions, rather than being passed to an offline conventional furnace. With the furnace immediately before the rolls, the material will receive both a recovery anneal as well as a reheat to allow continued warm rolling. Using a plasma arc lamp with a width of 1 cm and translated at 15 mm/s yielding about 1.5 s of heating resulted in recrystallization and a stress strain curve

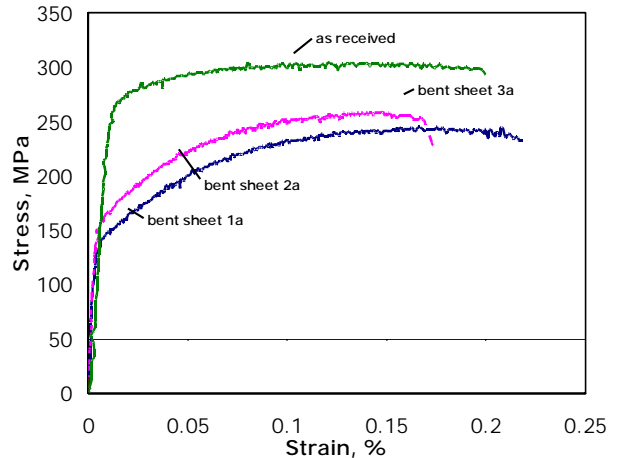


Figure 6. Tensile behavior from sheets processed by bending-unbending where sheet 1a was bent the most severely and sheet 3a the least. The resulting behavior is not dissimilar from a conventional annealed sheet.

equivalent to a standard furnace anneal for 1 h at 400°C (see the side views shown in Figure 7). Some surface crystallographic texture improvements were noted. Note that in Figure 7 there is a uniformity of grain size through the 3-mm thickness. Experiments have begun, using a bank of infrared heat lamps with 1 min. warm up and 1 min. at 400°C, prior to rolling. Figure 8 shows cross section optical micrographs at the top and at the bottom after a fifth warm rolling pass of 15% reduction and subsequent anneal of material with a final thickness of 2 mm. We have also observed that the textures of hot-rolled sheets have been significantly weaker than the material that we have obtained from the commercial vendor (Spectrulite). Incorporating radiant heating into the rolling process will probably result in a softer texture than that produced by conventional processing. This may result in a fringe benefit to the formability of the resulting sheet product.

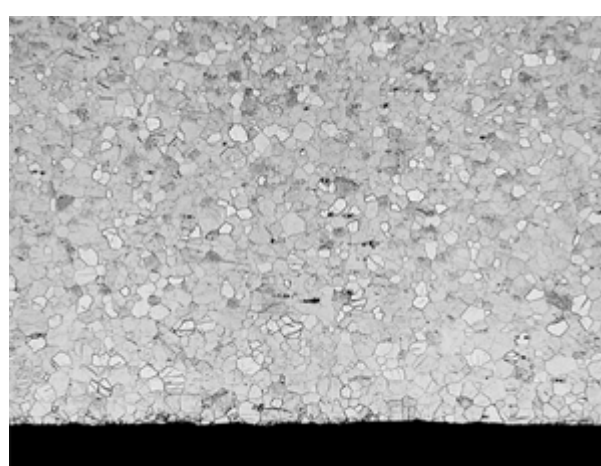
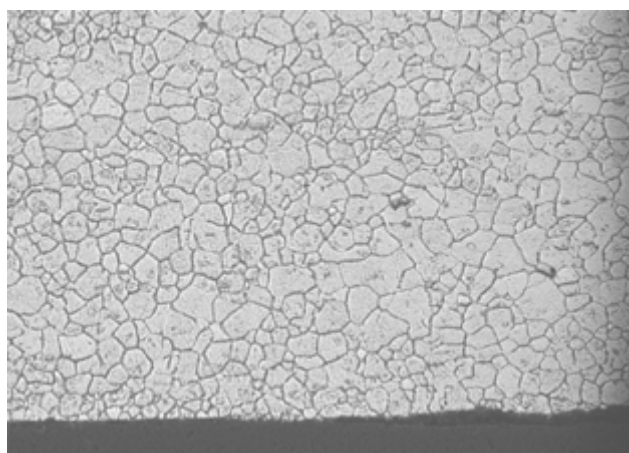
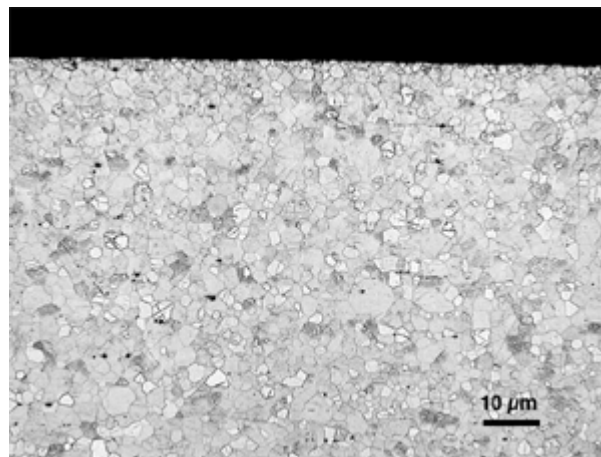
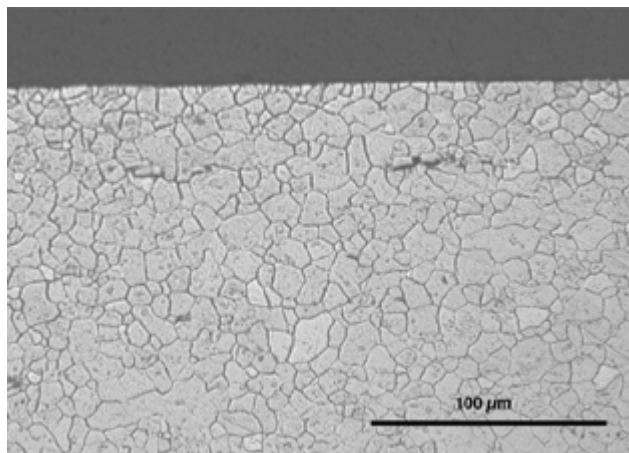


Figure 7. Optical micrographs from top and bottom of 3-mm-thick sheet of AZ31B with the H24 temper after approximately 1.5 s anneal from a plasma arc lamp translating at 15 mm/s at 500 W/cm². Recrystallization did occur from this brief anneal and was uniform through the thickness.

Figure 8. Optical micrographs after infrared lamp anneals from the top and bottom of AZ31B after the fifth anneal and 15% roll with a thickness of 2 mm. The anneals consisted of 1 min to heat up and 1 min. at 400°C. Again these micrographs show the uniformity of the microstructure through the thickness.

Evaluation of the Practical Formability (Deep Drawability) of New Alloys

During previous years, two alloy systems with exceptional ductility were identified. During FY 2003, we tested the practical formability by first warm rolling thin gage sheets from these alloys and then performing warm deep drawing experiments on these sheets. The Tinius Olsen formability tester with a cylindrical cup drawing die-set having a draw ratio of approximately 1.8 was used as a standard, and tests were performed at a range of punch speeds at temperatures

ranging from 100–200°C. Although one of the alloy classes had been reported to be cold rollable in an early publication, and the ductility had been observed to be quite good (Figure 9), we found the deep-drawing performance of WM3, WM4, and WM5 to be quite poor at all the rates and temperatures we explored (Figure 10). In contrast, we found the drawing performance of another alloy class to be superior to the industry standard AZ31 sheet material. Although AZ31B can be successfully deep drawn at

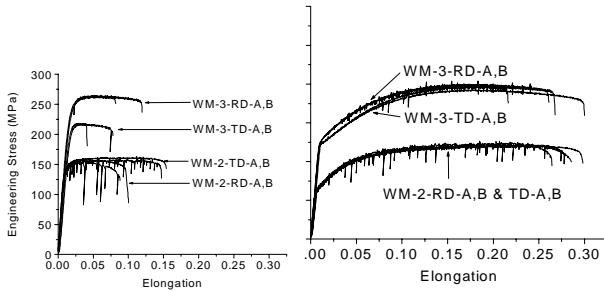


Figure 9. Tensile data from alloys WM2 and WM3 in the (a) as-rolled and (b) annealed conditions are representative of the two alloy classes investigated during our program. Both exhibit excellent ductility and little in-plane anisotropy in the annealed condition. Multiple curves for each sample type are shown.

150°C at low punch speeds (~2.5 mm/min), it is necessary to increase the temperature all the way to 200°C in order to achieve a perfect cup at the highest punch speed of ~250 mm/min. In the case of our experimental alloy WM2, a perfect cup can be drawn at the highest punch speed at only 150°C.

All of these results could be reconciled by examining the r-value of the various alloy sheets. The r-value is a measure of the sheet's anisotropy, specifically its resistance to thinning. A value of 1 means isotropy, and values above one mean a material that strongly resists thinning, while values below one mean a material which preferentially thins. Practical experience, particularly with steels, dictates that high r-values promote drawability. In the present case, it was found that alloys WM4 and WM5 have very low r-values, which is quite uncommon for magnesium sheets, while WM2 has an exceptionally high r-value (even in comparison with commercial AZ31, which has a high r-value, see Figure 11) Thus, the magnesium sheets with high r-values were found to perform the best during deep drawing trials.

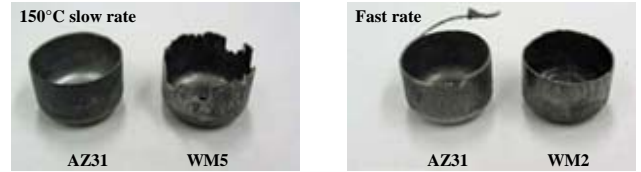


Figure 10. Cup drawing experiments demonstrate the practical formability of magnesium alloys. On the left, it is observed that AZ31 can be deep drawn at 150°C, while WM5 cannot be drawn successfully at any rate or temperature up to 200°C. At 150°C, alloy WM2 may be drawn at the fastest rate; however, AZ31 cannot be drawn at this rate until 200°C.

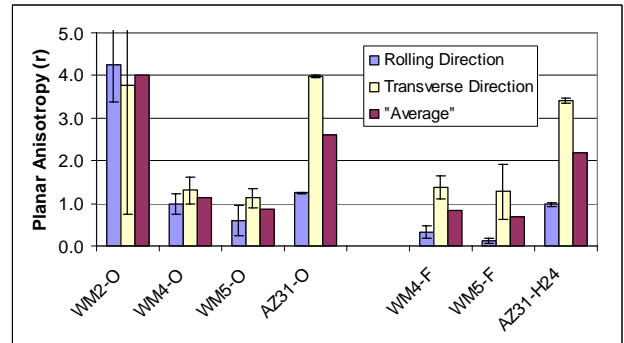


Figure 11. R-value measurements from various alloys, including the industry standard AZ31, in both the fully annealed O temper and the half-hard H24 temper.

During FY 2004, refinement of these alloys is planned to maximize their properties, including strength and ductility, and it is further planned to explore one more system involving dilute additions of zinc and rare earth elements.

Determination of Deformation Mechanisms Using Experimentation and Simulation

Correlating the crystallographic texture and deformation mechanisms with the anisotropy (or r-values) discussed above, led to the determination that magnesium sheets have high in-plane anisotropy (variation of the r-values within the plane of the sheet) at room temperature and that the specific deformation mechanisms and texture of

“cold-rolled” magnesium is responsible for this behavior. Polycrystal plasticity simulation reveals that primarily basal slip occurs during tension along the rolling direction, while prismatic slip is forced during tension along the transverse direction. Recent work using transmission electron microscopy has verified the occurrence of extensive nonbasal slip of $\langle a \rangle$ dislocations at room temperature.

During the past year, this understanding was extended to the high-temperature regime in an effort to understand why magnesium becomes so formable at even moderate forming temperatures. Again r-value measurement and simulation were used to determine the active deformation mechanisms. The r-values dropped precipitously with increasing temperature (Figure 12). Thus, counter to prior wisdom, the nonbasal (prismatic or pyramidal) slip of $\langle a \rangle$ type dislocations does not appear to be the main reason magnesium alloys become formable at moderate temperatures. We suggest that nonbasal slip of $\langle c+a \rangle$ type dislocations is responsible for the observed changes in r-value and formability.

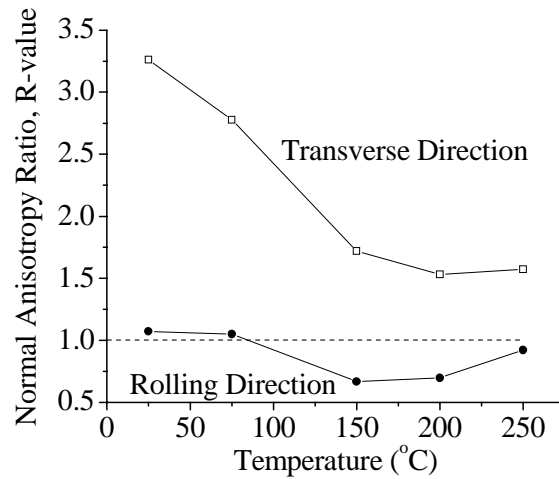


Figure 12. R-value measurements over a range of temperatures shows that the r-value drops strongly in all directions as the temperature is raised.

C. Equal Channel Angular Extrusion

Principal Investigator: R. B. Schwarz

Los Alamos National Laboratory

MST-8, Mail Stop G755, Los Alamos NM 87545

(505)667-8454; email: rxzs@lanl.gov

Co-Investigators: T. D. Shen, J. I. Archuleta

Technology Development Area Specialist: Sidney Diamond

(202) 586-8032; fax: (202) 586-1600; email: sid.diamond@ee.doe.gov

Field Technical Manager: Philip S. Sklad

(865) 574-5069; fax: (865) 576-4963; email: skladps@ornl.gov

Contractor: Los Alamos National Laboratory

Contract No.: W-31-109-Eng-38

Objective

- Conduct research on the theory, synthesis, and properties of soft ferromagnetic alloys having the potential to improve the efficiency of energy conversion devices in the U.S. transportation industry.

Approach

- Use mechanical alloying (MA) (a high-energy ball milling technique) to prepare Fe-rich alloy powders.
- Characterize the powder by X-ray diffraction, scanning differential calorimetry, and magnetometry.
- Consolidate the mechanically alloyed powders by equal-channel angular extrusion and spark-plasma sintering.
- Characterize the compacted alloys by ac and dc magnetic measurements.

Accomplishments

- Used MA to prepare magnetically soft Fe-Cu powders. We established optimal annealing parameters for reducing the residual stress in the Fe-Cu powders, while maintaining the crystallite size below 20 nm, as required for soft ferromagnetic properties. After reducing the residual stresses by annealing, the coercivity is approximately 0.5 Oe, and the saturation magnetization is 1.8 T.
- Studied Fe₈₀Cu₂₀ alloys that revealed the potential and limitations of the method.

Future Direction

- Study Fe-Al-Si alloys following the basic lines established in FY 2003.
 - Study the consolidation of our mechanically alloyed Fe-Al-Si powders by spark plasma sintering in collaboration with Professor A. K. Mukherjee at the University of California at Davis.
-

Introduction

The efficiency of electrical distribution grid systems can be increased by decreasing the power losses in step-up and step-down transformers. Because the amount of energy distributed by the grid is very large (3.8×10^{12} Wh for 2000 in the United States alone [1]), even a small increase in efficiency would represent a significant energy savings. Similarly, considerable savings can be achieved by increasing the efficiency of electric motors and other energy conversion devices used in the transportation industry.

Basic requirements for efficient cores in electromagnetic energy-conversion devices are low hysteresis losses and high saturation magnetization. Amorphous (glassy) ferromagnetic alloys are being studied for their potential in providing more efficient cores than those produced from conventional crystalline Fe(Si) alloys. Until recently, amorphous ferromagnetic alloys with coercivities in the tens of mOe [2] were only available as thin, glassy ribbons. These were produced by rapidly quenching a melt layer spread over a rotating copper wheel (melt spinning). To bypass crystallization during the quenching process, the melt must cool at a rate on the order of 10^6 K s^{-1} , which effectively limits the ribbon thickness to 30 to 50 μm . Because the resulting ribbon is so thin, a large number must be stacked to form the massive cores of transformers and motors. Such stacking inevitably leaves air gaps between the ferromagnetic foils, which decreases the packing density of the core. In turn, the low packing density requires longer copper-wire coils, resulting in increased Joule losses in the device. The optimal foil thickness is determined by a minimization of the combined core and Joule losses. An increase in the thickness of the ferromagnetic foils causes an increase in the core losses (due to higher eddy-current losses, which are proportional to the square of the foil thickness) but a decrease in the Joule losses due to a denser core. In

conventional power transformers made from crystalline Fe-3 wt % Si laminas (where the laminas can have any thickness), the optimum lamina thickness is about 300 μm . Although we have no equivalent study for amorphous ferromagnetic alloys, because amorphous alloys have higher resistivity than crystalline alloys, the optimal thickness for amorphous laminas is at least 300 μm , which is significantly thicker than that of ribbons formed by melt spinning.

Bulk Ferromagnetic Glasses

In the last decade, researchers have been able to prepare thicker amorphous alloy rods and laminas, which are now termed *bulk* metallic glasses [3-5]. Bulk metallic glasses are multicomponent alloys with particularly high values of the ratio T_g/T_l (between the glass-transition and liquidus temperatures), which enables bypassing crystallization during melt quenching at relatively low cooling rates. For example, a critical cooling rate of only 0.005 K s^{-1} has been measured in $\text{Pd}_{43.2}\text{Ni}_{8.8}\text{Cu}_{28}\text{P}_{20}$ alloy [6] and hence glasses of this composition can easily be prepared as 1-in.-diam rods or plates.

The optimal Fe-based compositions currently available for preparing bulk ferromagnetic alloys have critical cooling rates on the order of 10^2 K s^{-1} , making it possible to prepare 4- to 6-mm-thick glassy rods or plates [7,8]. Table 1 summarizes the properties of bulk Fe-based ferromagnetic glasses prepared in our laboratory. Although researchers have proposed various empirical rules for finding optimal compositions suitable for bulk glass production, no generally accepted theory exists for the selection of elements. We used the following reasoning. Because the product has to have a large Fe content, the glasses must belong to the metal-metalloid class of amorphous alloys. Starting with the known ferromagnetic glass $\text{Fe}_{80}(\text{P},\text{B})_{20}$ (which can

Table 1. Bulk ferromagnetic glassy rods (1 to 5 mm diam) prepared by flux melting and water quenching

Alloy	X	Density* (g/cm ³)	M _s * (T)	T _c * (°C)
(Fe ₄₀ Ni ₄₀)(100-x)/80(P ₁₄ B ₆) _{x/20} (x = 20-22)	20	7.61±0.01	0.87	268
Fe _{95-x} Mo ₅ (P ₁₃ C ₇) _{x/20} (x = 23 - 25)	24	7.45±0.01	0.96	160
Fe _{94-x} Mo ₄ Ga ₂ (P ₁₂ B ₄ C ₄) _{x/20} (x = 21- 23)	22	7.49±0.01	1.10	219
(Fe ₆₇ Cr ₄ Mo ₄ Ga ₄ B ₅ C ₅) _{(100-x)/89} P _x (x = 10 - 14.5)	12	7.51±0.01	-	162
(Fe ₆₆ Cr ₄ Mo ₄ Ga ₄ P ₁₂ C ₅) _{(100-x)/95} B _x (x = 3 - 6.5)	5.5	7.50±0.01	0.83	160
(Fe ₆₆ Cr ₄ Mo ₄ Ga ₄ P ₁₂ B ₅) _{(100-x)/95} C _x (x = 3 - 8.5)	6.5	7.48±0.01	0.84	153
Fe _{88-x} Cr ₄ Mo ₄ Ga ₄ (P ₁₂ B _{5.5} C ₅) _{x/22.5} (x = 20 - 22.75)	22.5	7.50±0.01	0.83	162
Fe _{77.5-3x} Cr _x Mo _x Ga _x P ₁₂ B _{5.5} C ₅ (x = 2.66 - 4.66)	2.66	7.43±0.01	1.07	213
Fe ₇₄ Mo ₄ P _{13.2} B _{4.4} C _{4.4}		7.44±0.02	-	198
Fe ₇₁ Cr ₄ Mo ₄ P ₁₁ B ₅ C ₅		7.43±0.02	0.87	126
Fe ₇₀ Co ₄ Mo ₄ P _{13.2} B _{4.4} C _{4.4}		7.52±0.01	1.17	233
Fe ₆₈ Co ₄ Mo ₄ Ga ₂ P _{13.2} B _{4.4} C _{4.4}		7.50±0.01	-	241
Fe ₆₅ Sb ₂ Cr ₄ Mo ₄ Ga ₄ P ₁₁ B ₅ C ₅		7.44±0.02	0.91	184
Fe ₆₂ Co ₅ Cr ₄ Mo ₄ Ga ₄ P ₁₁ B ₅ C ₅		7.43±0.02	0.86	171
Fe ₅₀ Co ₈ Ni ₈ Cr ₄ Mo ₄ Ga ₄ P ₁₂ B ₅ C ₅		7.60±0.02	-	180

* The glass properties in the last three columns are for the composition X given in the second column. M_s is the saturation magnetization and T_c is the Curie temperature.

only be prepared as a 30-μm-thick foil), we partially replaced Fe by elements such as Ni, Mo, Ga, Cr, Co, and Sb, all of which have different molar volumes than Fe, yet a near-zero heat of mixing with Fe. We avoided alloying with elements having a large positive or negative heat of mixing with Fe because such elements would have had a tendency either to phase segregate or to form ordered high-melting-temperature compounds. Melts containing elements of different molar volumes should be better packed and thus have higher viscosity, resulting in a lower critical cooling rate. Furthermore, crystal nucleation should be more difficult in multicomponent melts [9]. We optimized the alloy composition using the empirical criterion of correlating the glass formability with the difference $T_x - T_g$, where T_x is the crystallization temperature.

Figure 1 shows the dc hysteresis curve for Fe_{65.5}Cr₄Mo₄Ga₄P₁₂B_{5.5}C₅ glass. The M_s and T_c values of this glass and others prepared in this study are summarized in Table 1. Notice that M_s ranges from 0.83 to 1.17 T. These M_s values are lower than the M_s values of 2 T found in oriented Fe-3 wt % Si alloys. The Curie temperatures, T_c, of the bulk glasses are

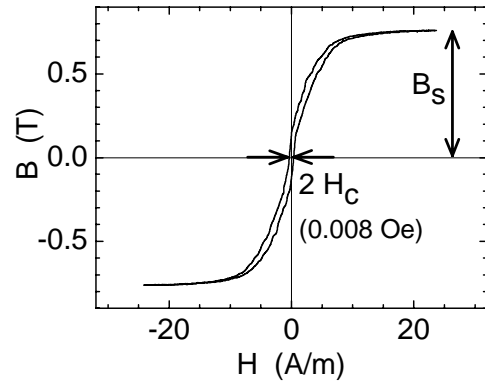


Figure 1. B-H curve measured on an amorphous Fe_{65.5}Cr₄Mo₄Ga₄P₁₂B_{5.5}C₅ toroid prepared from a 4-mm-diam glassy rod.

also rather low, ranging from 126 to 268°C. These relatively low M_s and T_c values result from alloying Fe with elements such as Cr and Mo, which is necessary to prepare bulk ferromagnetic glasses but also decreases the moment per Fe atom in the alloy. Because of their low M_s values, the glasses in Table 1 are not applicable to power transformers (which require M_s values of at least 1.5 T). However, these glasses have extremely low coercivity

and are thus potentially useful for sensor applications.

Figure 2 shows the ranges of M_s and H_c obtained for a variety of ferromagnetic alloys. It is apparent from this figure that the

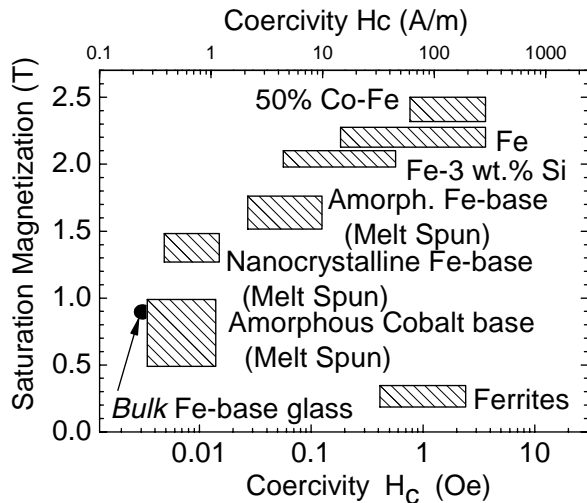


Figure 2. Ranges of saturation magnetization and coercivity in various soft ferromagnetic alloys.

lower H_c values (as required for low hysteresis losses) have been achieved at the expense of decreasing the M_s values. The current challenge is to develop materials having both low H_c and high M_s . So far, this goal has been approached most closely by two-phase materials consisting of nanosized *bcc* Fe particles embedded in an amorphous alloy matrix. Two nanocrystalline alloys, known under the trade names “Nanoperm” [10] and “Finemet” [11], are prepared by the partial crystallization of 30- to 50- μm thick rapidly quenched glassy ribbons. The saturation magnetization of these materials is approximately 1.4 T. Their main drawback is their thinness of gauge, which is not optimal for the construction of power transformers. In the next section we describe another approach to this problem, based on nanocrystalline ferromagnetic powders prepared by mechanical alloying.

Magnetic Properties of Nanocrystalline Ferromagnetic Alloys

The coercivity of crystalline alloys depends strongly on crystal size [12] because the magnetic domain walls interact with the grain boundaries. For decreasing grain size, H_c increases and reaches a maximum for grain sizes of approximately 100 nm. Further decreases in grain size lead to a rapid decrease in coercivity, in proportion to the sixth power of the grain size [13]. As the grain size approaches the exchange length, the averaged magneto-crystalline anisotropy of the randomly oriented crystallites offers no resistance to the Bloch walls, and the coercivity approaches the low value that is characteristic of amorphous ferromagnetic alloys. This feature of nanocrystalline ferromagnetic alloys has motivated extensive research of ferromagnetic powders prepared by MA. MA is a simple high-energy ball milling technique that was originally developed to prepare dispersion-strengthened Ni alloy powders [14]. Following MA, the dislocations in the heavily deformed particles are mainly concentrated at walls that delineate cells of lower dislocation density. The crystal size measured by X-ray diffraction corresponds to the size of these cells, which diffract semicoherently.

Table 2 summarizes the magnetic properties in mechanically alloyed powders reported in the literature. As can be seen in the table, none of these powders has a coercivity below 1 Oe, which is usually the value used to classify the material as magnetically soft. The lower half of Table 2 summarizes the magnetic properties of mechanically alloyed Fe-Cu powders. Fe and Cu have negligible solubility, yet, following extensive mechanical alloying, they form extended solid solutions: $\text{Fe}_{1-x}\text{Cu}_x$ is *fcc* for $0.4 < x < 1.0$, and *bcc* for $0 < x < 0.2$ [15]. Although most of these powders had crystallite sizes below 20 nm, the lowest H_c value reported in these works was 3.8 Oe. This is surprising since the Herzer plot [13]

predicts that for a crystallite size of 20 nm the coercivity should be in the 10^{-2} Oe range. This motivated us to reinvestigate the Fe-Cu system, especially the dependence of coercivity on annealing temperature.

We prepared $\text{Fe}_{80}\text{Cu}_{20}$ alloy powders by mechanically alloying mixtures of Fe and Cu powders in a SPEX-8000 mill using hardened steel vials. The milling charges were 8 g of powder and 32 g of $\frac{1}{4}$ -in.-diam H-440 steel balls. The weight of the powder recovered after 30 h of MA was within ± 0.1 g of the starting weight, and this indicated that the composition of the alloyed powder was within 1.5% of the starting composition.

Figure 3 shows X-ray diffraction patterns from mechanically alloyed $\text{Fe}_{80}\text{Cu}_{20}$ powder after annealing at the stated temperatures for

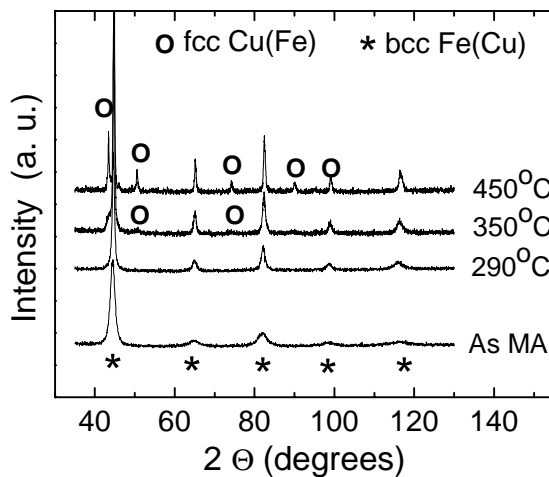


Figure 3. X-ray diffraction patterns of $\text{Fe}_{80}\text{Cu}_{20}$ powder prepared by mechanical alloying and after annealing for 1 h at various temperatures.

1 h. The as-processed powder is single-phase *bcc* and this metastable structure is preserved up to the annealing temperature of 290°C. Following anneals at higher temperatures, the alloy separates into Fe-rich *bcc* and Cu-rich *fcc* phases.

The influence of annealing temperature on coercivity, crystallite size, and root mean square (RMS) residual strain is shown in

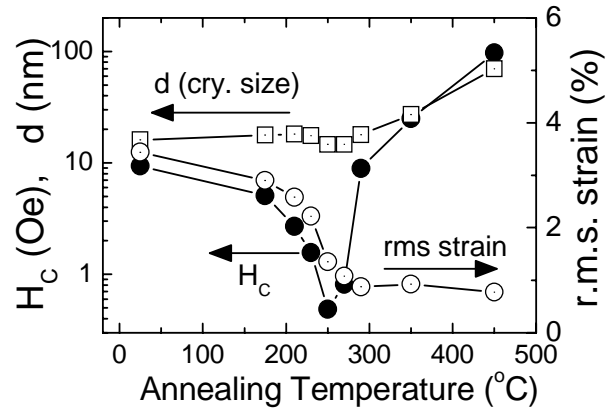


Figure 4. Coercivity, H_c , crystallite size, d , and RMS strain as a function of annealing temperature in mechanically alloyed $\text{Fe}_{80}\text{Cu}_{20}$ powder.

Figure 4. The crystallite size and the RMS strain were determined from the shapes of the Bragg peaks in Figure 3. Crystallite size is constant at 17 nm up to an annealing temperature of 290°C. However, for the same annealing temperature range, the RMS residual strain and H_c decrease significantly. The lowest coercivity (0.5 Oe) was obtained after annealing the $\text{Fe}_{80}\text{Cu}_{20}$ powder for 1 h at 250°C. Annealing at higher temperatures causes grain growth (as seen in Figure 4) and phase separation (as seen in Figure 3). Both effects increase H_c by providing additional obstacles to the motion of the domain walls. In the range 250 to 290°C, the crystallite size and the RMS strain remain approximately constant whereas H_c increases rapidly. This suggests that the coercivity increase is due mainly to phase separation, which is only detectable by X-ray diffraction at the higher annealing temperature of 350°C, when the volume fraction and domain size of the *fcc* phase are large enough to give a discernible X-ray signal. This study demonstrates that obtaining low H_c values in mechanically alloyed powder requires (1) starting from crystallite sizes below approximately 20 nm and (2) a careful annealing treatment that reduces the residual stresses while avoiding phase separation and grain growth. The saturation magnetization of the

Table 2. Coercivity in nanocrystalline alloy powders prepared by mechanical alloying

Material	Treatment	H _c (Oe)	Reference
Fe ₅₀ (SiC) ₅₀	MA (various times)	154–320	18
Fe-M (M=Zr,Hf,Co,Si)	MA & anneal	57–6.6	19
Fe _{100-x} M _x (M = Co or Ni, x = 0-100)	MA & anneal	5.1–56	20
Fe _{100-x} M _x (M = Al, Si, Cu, x = 0-50)	MA	3.8–50	21
Fe ₈₆ Zr ₇ B ₆ Cu ₁	MA + anneal	7.5	22
Fe ₈₆ Zr ₇ B ₆ Cu ₁	MA & anneal	14–7	23
Fe ₈₀ M ₁₀ C ₁₀ (M = Ta,Hf,W,Mo,Nb,Zr,Ti)	MA & anneal	194–3.8	24
Ni ₃ Fe	MA & anneal	22–7	25
Fe ₇₅ Al _{12.5} Ge _{12.5}	MA & anneal	37-21	25
Ni ₃ Fe	MA (various times)	33-73	26
Fe ₉₀ W ₁₀	MA (various times)	11–44	27
Fe _{100-x} Co _x (x = 0-80)	MA & anneal.	6.3–17	28
Fe _{100-x} Si _x (x = 0-40)	MA & anneal	74–2.4	29
Fe-(Co,Ni)-Zr-B	MA + anneal	15–44	30
Fe ₅₀ Cu ₅₀	as-MA	40	31
Fe ₅₀ Cu ₅₀	MA + anneal @ 820 K	300	31
Fe ₅₁ Cu ₄₉	as-MA	8	32
Fe ₅₁ Cu ₄₉	MA + anneal @ 723 K	640	32
Fe ₅₁ Cu ₄₉	MA + anneal @ 923 K	200	32
Fe ₅₀ Cu ₅₀	MA (140 h)	110	33
Fe ₅₀ Cu ₅₀	MA (440 h)	29	33
Fe ₅₀ Cu ₅₀	MA + anneal @ 600 K	29–160	34
Fe ₅₀ Cu ₅₀	as-MA	316	35
Fe ₆₆ Cu ₃₄	as-MA	289	35
Fe ₇₅ Cu ₂₅	as-MA	273	35
Fe ₉₀ Cu ₁₀	as-MA	258	35

18. T. D. Shen, K. Y. Wang, M. X. Quan, and J. T. Wang, *J. Mater. Sci. Lett.* **11**, 1576 (1992).
 19. N. Kataoka, K. Suzuki, A. Inoue, and T. Masumoto, *J. Mater. Sci.* **26**, 4621 (1991).
 20. C. Kuhrt and L. Schultz, *J. Appl. Phys.* **73**, 6588 (1993).
 21. C. Kuhrt and L. Schultz, *IEEE Trans. Magn.* **29**, 2667 (1993).
 22. R. Schäfer, S. Roth, C. Stiller, J. Eckert, U. Klement, and L. Schultz, *IEEE Trans. Magn.* **32**, 4383 (1996).
 23. C. Stiller, J. Eckert, S. Roth, R. Schäfer, U. Klement, and L. Schultz, *Mater. Sci. Forum* **225-227**, 695 (1996).
 24. C. Kuhrt, *J. Magn. Magn. Mater.* **157/158**, 235 (1996).
 25. H. N. Frase, R. D. Shull, L. B. Hong, T. A. Stephens, Z. Q. Gao, and B. Fultz, *NanoStru. Mater.* **11**, 987 (1999).
 25. C. N. Chinnasamy, A. Narayanasamy, K. Chattopadhyay, and N. Ponpandian, *NanoStru. Mater.* **12**, 951 (1999).
 26. M. Kis-Varga, D. L. Beke, and L. Daróczy, *Mater. Sci. Forum* **343-346**, 841 (2000).
 27. Y. D. Kim, J. Y. Chung, J. Kim, and H. Jeon, *Mater. Sci. Eng. A* **291**, 17 (2000).
 28. J. Ding, Y. Li, L. F. Chen, C. R. Deng, Y. Shi, Y. S. Chow, and T. B. Gang, *J. Alloys Comp.* **314**, 262 (2001).

29. Y. J. Liu, I. T. H. Chang, and M. R. Lees, *Scripta Mater.* **44**, 2729 (2001).
30. A. Hernando, P. Crespo, J. M. Barabdiaran, A. García Escorial, and R. Yavari, *J. Magn. Magn. Mater.* **124**, 5 (1993).
31. P. Crespo, A. Hernando, R. Yavari, O. Drbohlav, A. García Escorial, J. M. Barabdiarán, and I. Orúe, *Phys. Rev. B* **48**, 7134 (1993).
32. O. Drbohlav and A. R. Yavari, *J. Magn. Magn. Mater.* **137**, 243 (1994).
33. O. Drbohlav and A. R. Yavari, *Acta Metall. Mater.* **43**, 1799 (1995).
34. B. Majumdar, M. M. Raja, A. Narayanasamy, and K. Chattopadhyay, *J. Alloys Comp.* **248**, 192 (1997).

mechanically alloyed Fe₈₀Cu₂₀ powder, measured on a SQUID apparatus at an applied field of 50 kOe, was 1.8 T. M_s remained approximately constant during the annealing treatment.

To prepare laminas of potential use in the manufacture of transformers, the mechanically alloyed Fe₈₀Cu₂₀ powder must be consolidated into fully dense laminas. Residual porosity will create pinning centers and thus will increase the coercivity and decrease the permeability of the laminas. Achieving full density is difficult because the mechanically alloyed Fe₈₀Cu₂₀ particles have high hardness, in excess of 5 GPa [16], and the consolidation must be done at $T < 250^\circ\text{C}$. We investigated the consolidation of the mechanically alloyed Fe₈₀Cu₂₀ powder by ECAE. This technique consists of pushing a square cross-section ingot through a die having a 90-degree bend. At the bend, the ingot is sheared by 100%. Because the ECAE extrusion preserves the cross section of the product, repeated shearing can be used to accumulate larger strains. In a previous study, we demonstrated that mixtures of Cu and Ag powders consolidated by ECAE were 100% dense [17].

We encapsulated the as-mechanically alloyed Fe₈₀Cu₂₀ powder in $0.9 \times 0.9 \times 4 \text{ in.}^3$ copper cans. Lids were sealed to the cans by e-beam welding. The encapsulation process was done inside an Ar-filled glovebox (oxygen content below 1 ppm) to avoid exposing the powder to air. Each copper can containing the powder was given a single ECAE pass at room temperature, after which the compacted Fe₈₀Cu₂₀ ingot was removed by machining away the Cu can. The relative density of the ECAE-compacted powder was

only 72%. This low relative density was attributed to the elevated hardness of the mechanically alloyed Fe₈₀Cu₂₀ powder. As a consequence, during ECAE the particles tend to roll past each other rather than deform and cold weld, as is the case when extruding mixtures of low-hardness Cu and Ag powder. A small toroid-shape ferromagnetic core was fabricated from this ECAE ingot, to which we added primary and secondary coils. The miniature transformer was then annealed at 260°C for 1 h.

Figure 5 shows the dc hysteresis curve measured on the toroidal core made from Fe₈₀Cu₂₀ consolidated by ECAE. The hysteresis curve is almost closed, except at low values of the applied field, where the hysteresis curve opens, giving a coercivity of 4 Oe. The area inside the hysteresis curve is 10680 Gauss·Oe. This product corresponds to an energy loss per cycle of 0.125 J/kg. The low permeability of the material, approximately $25 \mu_0$, is a direct consequence of its low relative density. This material has potential use for the manufacture of magnetic chokes and transformers for flyback converters, especially if the hysteresis losses are further reduced by removing the residual macrostresses developed during the toroid manufacture.

Discussion

Bulk ferromagnetic metallic glasses of the type Fe- M - m , where M is one or more of the transition metals Co, Ni, Ga, Cr, Mo, and m is a metalloid such as B, P, or C, exhibit excellent magnetic properties, especially extremely low coercivity. The main

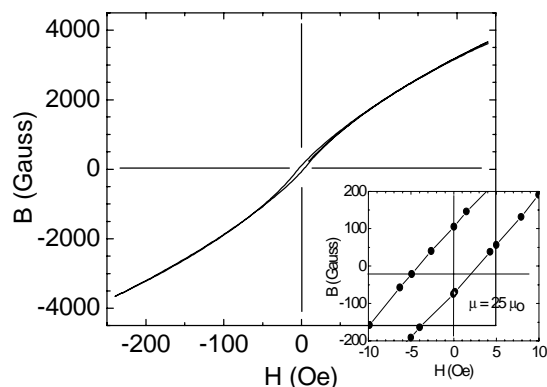


Figure 5. Hysteresis B-H curve for mechanically alloyed Fe₈₀Cu₂₀ powder consolidated by equal-channel angular extrusion and annealed for 45 min at 160°C.

limitation of these bulk ferromagnetic glasses is their relatively low saturation magnetization (about half that of oriented polycrystalline Fe-3 wt % Si). Researchers are investigating bulk glasses that contain no Cr or Mo, because these elements lower the Curie temperature [18,19] and thus also lower the saturation magnetization at near room temperature. The extremely low coercivity of the present bulk glasses, coupled with their good mechanical strength (which was not discussed here) makes them attractive for applications such as sensors, magnetic delay lines, and transducers.

Although bulk glasses and crystalline alloys have quite different short-range ordering, amorphous alloys exhibit long-range ferromagnetic ordering. As for crystalline alloys, the magnetic behavior of amorphous alloys depends strongly on residual strain. Obtaining coercivities in the range of 10⁻³ Oe requires removing residual stresses developed during the quenching process. The same is true for nanocrystalline alloys. Nanocrystalline Fe₈₀Cu₂₀ powders prepared by MA have low coercivity only after most of the residual stress has been reduced by annealing. The annealing temperature-time window is rather narrow because the bcc Fe₈₀Cu₂₀ alloy is metastable and thus tends to phase separate. Annealing the powder removes microstresses, those

existing within each powder particle. After the powder has been consolidated into laminas or toroids, the product also has macro stresses. It is unlikely that long-range residual stresses can be effectively reduced by annealing within the same temperature window used to reduce the microstresses. Future research in this field should address alloy compositions such as Fe_(1-x-y)Al_xSi_y, where x and y can be chosen to minimize the magnetostriction.

Acknowledgement

This work was supported by the Office of FreedomCar and Vehicle Technologies of the U.S. Department of Energy.

References

1. U.S. Department of Energy "Annual Energy Review 2001," from www.eia.DOE.gov.
2. R.C. O'Handley, L.I. Mendelsohn, R. Hasegawa, R. Ray, and S. Kavesh, *J. Appl. Phys.* **47**, 4660 (1976).
3. A. Inoue, K. Ohtera, K. Kita, and T. Masumoto, *Jap. J. Appl. Phys.* **27**, L2248 (1988).
4. A. Peker and W. J. Johnson, *Appl. Phys. Lett.* **63**, 2342 (1993).
5. Y. He, J. I. Archuleta, and R. B. Schwarz, *Appl. Phys. Lett.* **69**, 1861 (1996).
6. T. D. Shen and R. B. Schwarz, unpublished results, Los Alamos National laboratory, 2003.
7. A. Inoue and J. S. Gook, *Mater. Trans. JIM* **36**, 1180 (1995).
8. T. D. Shen and R. B. Schwarz, *Appl. Phys. Lett.* **75**, 49 (1999).
9. A. L. Greer, *Nature* **366**, 303 (1993).
10. A. Kojima, H. Horikiri, Y. Kamamura, A. Makino, A. Inoue, and T. Matsumoto, *Mater. Sci. Eng. A* **179/180**, 511 (1994).
11. Y. Yoshizawa, S. Oguma, and K. Yamauchi, *J. Appl. Phys.* **64**, 6044 (1988).
12. R. M. Bozorth, "Ferromagnetism," van Nostrand, New York (1951).

13. G. Herzer, *Scripta Metall. Mater.* **33**, 1741 (1995).
14. J. S. Benjamin, *Sci. Amer.* **234**, 40 (1976).
15. J. Eckert, R. Birringer, J. C. Holzer, C. E. Krill, and W. E. Johnson, *Mat. Res. Soc. Symp. Proc.* **238**, 739 (1992).
16. T. D. Shen and C. C. Koch, *Acta Mater.* **44**, 753 (1996).
17. R. B. Schwarz, J. I. Archuleta, G. Korth, J. Macheret, and T. Lillo, unpublished results, Los Alamos National Laboratory (2002).
18. M. Oliver, J. O. Strom-Olsen, and Z. Altounian, *Phys. Rev. B* **35**, 333 (1987).
19. H. J. V. Nielsen, *Solid State Comm.* **30**, 239 (1979).

D. Equal Channel Angular Extrusion Processing of Alloys for Improved Mechanical Properties

Principal Investigator: Thomas M. Lillo
Idaho National Engineering and Environmental Laboratory
MS2218, P.O. Box 1625, Idaho Falls, ID 83415-2218
(208)526-9746; fax: (208)526-4822; e-mail: tml@inel.gov

Technology Development Area Specialist: Sidney Diamond
(202) 586-8032; fax: (202) 586-1600; e-mail: sid.diamond@ee.doe.gov
Field Technical Manager: Philip S. Sklad
(865) 574-5069; fax: (865) 576-4963; e-mail: skladps@ornl.gov

Contractor: Idaho National Engineering and Environmental Laboratory
Contract No.: DE-AC07-99ID13727

Objective

- Investigate equal channel angular extrusion (ECAE) as a deformation processing technique to improve material properties such as strength, formability, fatigue, and corrosion properties.
- Produce advanced, lightweight materials with enhanced formability, higher strength-to-weight ratio, and higher stiffness, ultimately leading to reductions in vehicle weight and thus more fuel-efficient vehicles.

Approach

- Modify the existing ECAE die at Idaho National Engineering and Environmental Laboratory and the furnace design as necessary to allow processing of a magnesium alloy (ZK60A) and an aluminum metal matrix composite (AL6061+B₄C).
- Use ECAE to process materials and a variety of ECAE processing parameters such as processing temperature, number of passes through the die, processing route, and processing speed.
- Characterize the microstructure and mechanical properties of the ECAE-processed material.
- Use microstructure and mechanical property data to model the flow stress of materials processed with ECAE.

Accomplishments

- Modified ECAE die to allow the application of a back stress in the material during ECAE processing.
- Used ECAE to process ZK60A and AL6061+10 wt % B₄C materials under a variety of conditions.
- Characterized microstructure and mechanical properties of ECAE-processed material.
- Characterized mechanical properties of various brasses that had been ECAE processed and annealed in support of flow-stress modeling work.

Future Direction

- Optimize ECAE parameters for ZK60A alloy to obtain maximum superplastic behavior.

- Optimize ECAE parameters for AL6061 + B₄C composites to uniformly distribute the B₄C particulate in the alloy and maximize room temperature ductility.
- Modify ECAE furnace and ECAE process a titanium alloy and titanium alloy composite for increased ductility.
- Continue ECAE processing of materials and their characterization in support of flow-stress modeling.

Introduction

The weight of a structural component is determined by the load it must withstand and the yield strength of the material from which it is made. Materials with a higher strength-to-weight ratio can significantly reduce the weight of structural components in vehicles and provide increased fuel efficiency. In general, the strength of metals and alloys can be increased through reductions in the scale of the microstructure (e.g., grain size, second phase particles). Deformation processing (e.g., rolling, forging) increases strength but also reduces ductility. An annealing heat treatment is often required to bring the material back to a state of reasonable ductility at the expense of a slight reduction in yield strength. Materials subjected to higher levels of deformation strain can be annealed at lower temperatures and possess a finer final grain size and high yield strength. The goal of this project is to use deformation processing to develop high-strength, lightweight materials with reasonable ductility for applications in vehicles. This type of processing will reduce overall vehicle weight and, thereby, improve fuel efficiency.

ECAE is a relatively new deformation processing technique that imparts a great deal of deformation to a work piece without changing the cross-section of the work piece. The work piece enters the ECAE die and is forced into the exit channel (having the same dimensions as the entrance channel) that is at some prescribed angle to the entrance channel, typically 90° (see Figure 1). As the work piece moves from the entrance channel to the exit channel it undergoes a large

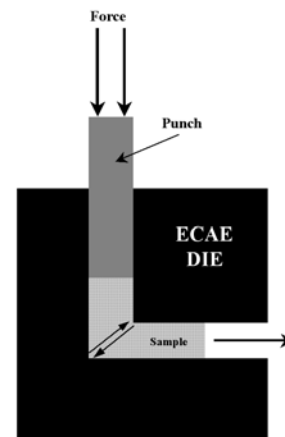


Figure 1. Schematic of ECAE processing.

amount of deformation strain (approaching $e = 1$, for a 90° intersection of the entrance and exit channels). Because the cross-section remains unchanged, it can be passed through the die repeatedly to accumulate strains greater than $e = 20$. The thickness of a material would have to be reduced by >99% to achieve a similar strain level by conventional rolling. Furthermore, since the cross-section remains relatively unchanged, the sample can be rotated prior to subsequent passes to obtain different strain paths and potentially different final microstructures and properties (see Figure 2).

ECAE processing of simple metals and alloys was investigated during the previous years of this project. The goal of those investigations was to gain an understanding of the ECAE process and the effect of the various ECEA-processing parameters on the

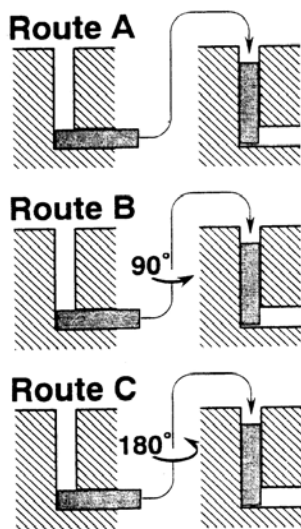


Figure 2. Schematic illustrating sample rotation between subsequent passes through the ECAE die.

resulting microstructure and mechanical properties. The main conclusions revealed by those studies were

- The microstructure is drastically affected during initial passes through the ECAE die and reaches, more or less, a steady state configuration after four passes.
- The route used during multiple-pass ECAE processing produced only small differences in microstructure and mechanical properties.
- ECAE processing could be used to impart high strains ($\epsilon > 10$) to ductile materials.
- Recrystallization of ECAE-processed materials occurred at relatively low temperatures and, typically, the recrystallized grain size was on the order of $1 \mu\text{m}$.
- Materials with a low-to-moderate stacking fault energy recrystallized with a very high fraction of twin-related grains (approaching 50%).

- The microstructure of commercially pure metals could not be refined into the nanocrystalline regime by ECAE processing.
- Microstructure developed by the formation of dislocation subcells. The misorientation across the subcell boundaries increased as the number of passes through the ECAE die increased. The development of high-angle grain boundaries required a high number of passes (>10) through the ECAE die.
- Materials of limited ductility tend to fail during ECAE process by either cracking or macroscopic shear banding.
- Finite element modeling (FEM) of the ECAE process shows that significant tensile forces develop on the upper surface of the sample and can cause cracking.
- Application of a back stress on the exiting sample reduces the magnitude of the tensile stresses. If the back stress is large enough, low ductility samples can be ECAE processed without failure.
- Back stress allows the ECAE processing temperature to be lowered, resulting in greater microstructural refinement.

Based on these conclusions, the research during FY 2003 was focused on lightweight alloys with potential vehicle applications. Such alloys typically suffer from low stiffness and formability. The magnesium alloy, ZK60A, was chosen for study with the goal of developing a superplastic material for low-temperature, high strain rate forming. ECAE-processing of this alloy at relatively low temperature ($\sim 150^\circ\text{C}$) with back stress resulted in a very uniform and fine microstructure with a grain size on the order of $1\text{--}2 \mu\text{m}$. The superplastic properties were investigated during FY 2003.

The other material studied during FY 2003 was an aluminum alloy metal matrix composite, AL6061+B₄C particulate. Particulate metal matrix composites are made by either consolidation of powders or through additions of particulate to the molten matrix,

which is then solidified. Inhomogeneous distribution of the particulate phase result in poor ductility and an elastic modulus that is less than that predicted by the rule of mixtures. The high-shear strains in ECAE processing should be able to break up agglomerates of particles and redistribute them more evenly throughout the matrix, with a significant improvement in elastic modulus and ductility.

Work in support of the effort to model the flow stress of metals and alloys also continued during FY 2003. It was realized early on in this project that ECAE could be used to produce very fine grain-size materials—finer than previously obtained by rolling, for instance. This afforded the opportunity to study the relationship between flow stress and grain size at previously unobtainable small values of grain size. The relationship was studied over a wide range of grain sizes (2–200 μm). It was expected that the flow stress would depend on reciprocal square root of the grain size, in accordance with theories of grain boundaries as barriers to dislocation movement (i.e., Hall-Petch theory) or as sources for dislocations (theories of Li, Price, and Hirth). However, the flow-stress data for the wider range of grain sizes studied in this work suggested flow stress varied as the reciprocal of grain size and not the reciprocal square root of grain size. A better fit to the data was obtained when the flow stress was plotted against reciprocal of twin grain-boundary spacing suggesting twin grain boundaries were acting as the source of dislocations. The main conclusion of that work is that grain size is only important at the onset of plastic flow and that subsequent strain hardening is independent of grain size; that is, grain boundaries provide an initial source of dislocations but do not participate in strain hardening, only dislocation or dislocation interactions produce strain hardening. A series of brasses, with systematically varying stacking fault energy were ECAE processed, annealed, and evaluated for mechanical properties in support of the modeling work of flow stress.

ECAE Processing of Magnesium Alloys

Two magnesium alloys were used for this study, one was commercial grade ZK60A (Mg-5% Zn – 0.5% Zr) and an experimental magnesium alloy provided by Dr. Daniel Shechtmen, located at the National Institute of Standards and Technology (NIST). (Dr. Shechtmen's alloy is basically ZK60A with additions of 0.5 wt % Ce and 0.5 wt % Y. These additions result in the formation of quasi-crystals that strengthen the alloy.) The goal for the commercial ZK60A was to reduce the grain size to obtain superplastic properties; while the goal for the Shechtmen alloy was to break up and redistribute the quasi-crystalline phase.

Commercial ZK60 samples were ECAE processed using three different sets of parameters:

- 4 passes by the B-route at 260°C and no applied back stress
- 4 passes by the B-route at 150°C and 18.3 ksi back stress
- 6 passes by the B-route at 150°C and 18.3 ksi back stress

The ECAE processing temperature had to be raised to 260°C on the first sample to avoid failure of the billet during processing without back stress. Figure 3 compares the microstructure as a function of temperature. It is obvious from this figure that ECAE leads to a refinement in microstructure with the refinement being more dramatic at lower processing temperatures. The application of a back stress allowed processing at lower temperatures to obtain greater microstructural refinement.

Table 1 shows the results of elevated temperature tensile tests on the ECAE-processed and as-received ZK60A for two relatively rapid strain rates, $10^{-3}/\text{s}$ and $10^{-2}/\text{s}$. The as-received material does not show extensive ductility at a strain rate of $10^{-3}/\text{s}$. ECAE processing increases the ductility

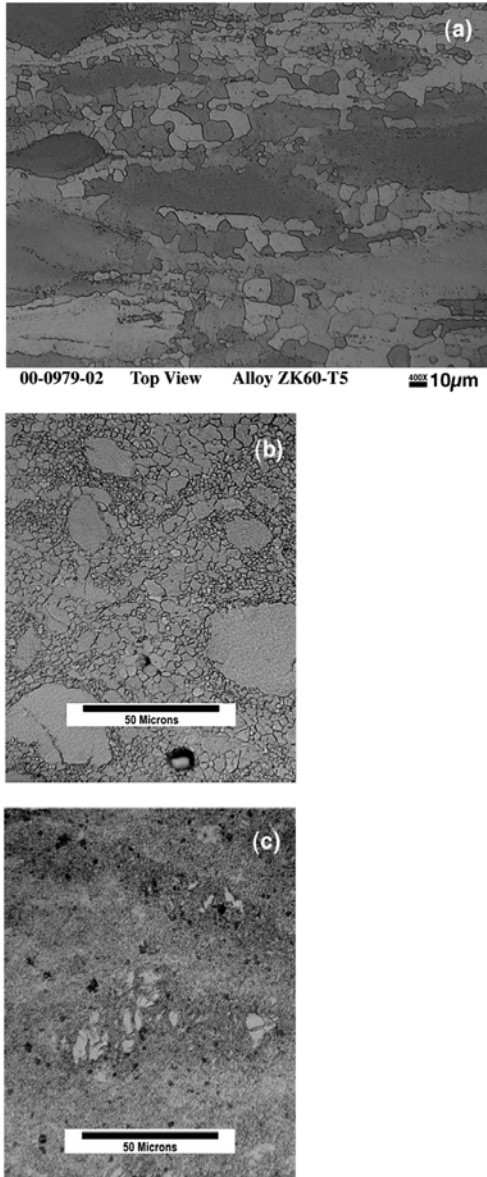


Figure 3. Effect of ECAE processing on the microstructure of commercial ZK60A.

significantly. Increasing the number of passes through the ECAE and lowering ECAE processing temperature results in increased ductility at a strain rate of $10^{-3}/s$. This can be directly related to the greater microstructural refinement obtained at lower ECAE processing temperatures, shown in Figure 3. The values for ductility at 200°C are somewhat lower

Table 1. Tensile properties of ECAE-processed, commercial ZK60A at 200°C

	As-received	4B, 260°C, 0 ksi	4B, 150°C, 18.2 ksi	6B, 150°C, 18.2 ksi
Strain rate = $1 \times 10^2/s$				
Yield strength, MPa	N/A	84	70	65
UTS	N/A	95	73	71
Ductility	N/A	87	142	121
Strain rate = $1 \times 10^3/s$				
Yield strength, MPa	115	77	28	32
UTS	130	78	33	51
Ductility	60	91	60*	223

*Sample failed prematurely at an internal flaw

than found in the literature (422% at $10^{-3}/s$ by H. Wantanabe, et al.)¹ for ZK60-processed 8B passes at 160°C. It is assumed that the higher number of passes in that work is responsible for the greater ductility.

The results of ECAE processing the modified ZK60A alloy containing quasi-crystals followed those of the commercial ZK60A. However, ECAE processing was modified to account for the increased strength of this alloy. The first two passes were carried out at 250°C with 9.8 ksi back stress to break up the quasi-crystalline phase on the grain boundary. The ECAE processing temperature was then lowered (200°C with 11.2 ksi back stress) for the remaining four passes to further refine the microstructure. Figure 4 shows the microstructure (a) before and (b) after ECAE processing. The quasi-crystalline phase is the bright phase in these photomicrographs. ECAE processing of this alloy resulted in the break up and redistribution of the quasi-crystalline grain boundary phase. Quasi-crystalline particles located at the interior of the grains seemed to be unaffected by ECAE processing. Additional reduction of the ECAE temperature is expected to aid in the break up and redistribution of the quasi-crystalline phase.

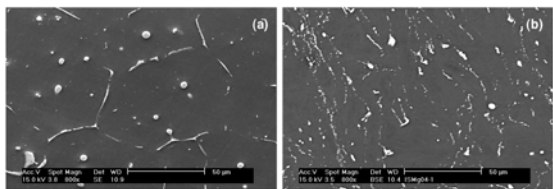


Figure 4. Microstructure of modified ZK60A containing quasi-crystals, as-received (left) and after ECAE processing.

Table 2 shows that the elevated temperature tensile properties of the modified ZK60 alloy exceed those of the commercial ZK60A material (see Table 1 for comparison). The presence of the quasi-crystalline phase increased the strength of the alloy by almost a factor of two. The modified alloy also exhibits greater ductility (~35% greater at 10^{-2} /s and ~14% at 10^{-3} /s). It appears that this alloy has a better potential for high strain rate superplasticity. ECAE processing parameters will be optimized during FY 2004.

Table 2. Tensile properties of ECAE-processed, modified ZK60A (w/quasi-crystals) at 200°C

ECAE conditions	2B, 250°C, 9.8 ksi + 4B, 200°C, 11.2 ksi
Strain rate = 1×10^{-2}/s	
Yield strength, MPa	115
UTS, MPa	124
Ductility, %	185
Strain rate = 1×10^{-3}/s	
Yield strength, MPa	56
UTS, MPa	72
Ductility, %	260

ECAE Processing of Aluminum Alloy Composites

Prototype metal matrix composites were purchased from Dynamet Technology, Inc. The material consisted of an Al6061 matrix with boron carbide particles (~50 μm in diameter on average) present at a level of either 10 or 20 wt %. Additions of ceramic particles increase the stiffness of the AL6061 matrix, making it more suitable for use in lightweight structural applications. The material was fabricated by powder metallurgy

methods and contained agglomerates of boron carbide particles. The B_4C particles appeared to be concentrated around prior aluminum alloy powder particles (see Figure 5a). The interface between adjacent B_4C particles is very weak and acts as a defect during tensile loading, causing premature fracture. The elongation/ductility of these composites is negligible in the as-received state. ECAE processing (4A passes at 300°C, no back stress, and 4A passes at 150°C and 21 ksi back stress) was performed to break up B_4C agglomerates and isolate the particles in the AL6061 matrix.

Figure 5 shows the effect of ECAE processing on the B_4C distribution. Relatively

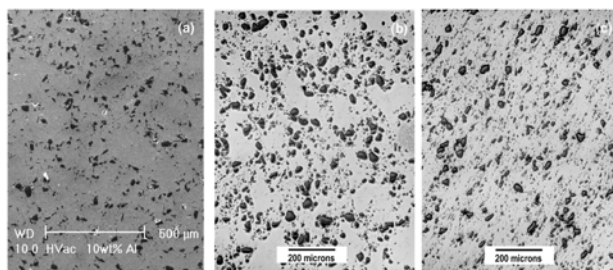


Figure 5. Microstructure of AL6061 + 10 wt % B_4C .

high processing temperatures are required to prevent billet failure (i.e., cracking or shear failure) if a back stress is not imposed on the billet during ECAE processing. The high processing temperature increases the ductility but also reduces the strength of the matrix. The results suggest that the very hard particles are rolling in a soft matrix, somewhat analogous to marbles in bread dough. During deformation, the marbles simply get pushed around in the dough. If the temperature is lowered and a back stress is imposed, the strength of the matrix increases and greater load transfer to the hard particles occurs. The result is better distribution of the particles in the boron carbide agglomerates (see Figure 5, the 4A, 150°C, 21 ksi sample). It also appears that ECAE processing at low temperature with a back stress has closed residual porosity observed in the as-received material.

Table 3 shows the tensile properties of the ECAE-processed samples. The as-received

Table 3. Tensile properties of ECAE-processed AL6061 and AL6061+10 wt % B_4C

		AL6061-T4 (no B_4C)	
ECAE conditions		4A, 24°C, 0 ksi	4A, 300°C, 0 ksi
Yield strength, MPa		130	116
Ultimate strength, MPa		250	242
Elongation, %		37.5	41.8
Density*, g/cm³ (%)		N/A	N/A
Elastic modulus**, MPa		N/A	N/A
		AL6061+10 wt % B_4C -T4	
ECAE conditions		4A, 300°C, 0 ksi	4A, 150°C, 21 ksi
Yield strength, MPa		130	146
Ultimate strength, MPa		209	250
Elongation, %		6.0	12
Density*, g/cm³ (%)		2.61 (97)	2.56 (95)
Elastic modulus**, MPa		75400	78,600

* Theoretical density of AL6061+10 wt % B_4C is 2.69 g/cm³.

**Elastic modulus for commercial AL6061-T4 is 70250 MPa, and the theoretical modulus for AL6061+ 10 wt % B_4C is ~110,000 MPa.

material broke during machining of tensile bars, suggesting that the as-received material has very poor properties. The tensile bars of the ECAE-processed material were heat treated on the B_4C distribution can be directly assessed. The table suggests that ECAE processing returns the yield and ultimate tensile stresses back to at least the values of commercial AL6061 without particulate additions. The composite still exhibits significantly less ductility than AL6061, but it is significantly more ductile than most metal matrix composites that typically exhibit insignificant ductility. Furthermore, Table 3 shows that higher ECAE processing

temperatures are better for eliminating residual porosity, thereby increasing the density, but results in a lower elastic modulus than ECAE processing at lower temperatures. (The elastic modulus was determined by ultrasonic techniques.) However, it should be noted that the elastic modulus still is well below the theoretical elastic modulus of ~110,000 MPa determined with the rule-of-mixtures. Therefore, it appears that an ECAE-processing scheme utilizing initial passes at relatively high temperature followed by passes at lower temperatures may optimize density and elastic modulus.

The results have intrigued Dynamet Technology, Inc., and it is providing more material at cost for FY 2004. If further results on the AL6061+ B_4C system support the results presented here, it wishes to explore ECAE processing on titanium alloy metal matrix composites for structural applications.

Modeling Flow Stress

Work in support of flow-stress modeling consisted mainly of tensile testing of materials previously ECAE processed. The effect of twin grain-boundary content on flow-stress behavior was investigated by ECAE processing commercially pure copper at different temperatures by the same route (4 passes by a modified B route with an applied back stress). Tensile specimens were then fabricated and annealed at various temperatures. Table 4 presents the tensile results, ECAE-processing conditions, and the annealing temperatures. Generally, higher ECAE-processing temperatures lower yield strength. The grain size and twin grain-boundary density remain to be characterized before the tensile results can be fully analyzed.

Also the effect of stacking fault energy on flow-stress behavior was studied. During FY 2003 two ECAE-processed brasses with 5 and 10% Zn, respectively, were evaluated for tensile properties. Billets of each composition were subjected to ECAE processing with and

Table 4. Tensile properties of ECAE-processed copper

Sample ID	ECAE conditions	Annealing temperature, °C	Yield strength, MPa	Ultimate strength, MPa	Elongation, %
Cu140	24°C, 4 pass, 5.6 ksi	None	405	431	23
-1	"	300	115	252	63
-2	"	400	54	228	60
-3	"	500	27	224	65
Cu141	125°C, 4 pass, 5.6 ksi	None	378	398	20
-1	"	300	110	247	63
-2	"	400	60	236	60
-3	"	500	30	219	75
Cu142	150°C, 4 pass, 5.6 ksi	None	353	374	23
-1	"	300	97	247	58
-2	"	400	63	230	60
-3	"	500	28	220	73
Cu143	225°C, 4 pass, 5.6 ksi	None	223	291	34
-1	"	300	71	239	65
-2	"	400	54	226	65
-3	"	500	27	224	87

without back stress. ECAE processing corresponded to one of the two following processing schemes:

- 2C passes @ 24°C, anneal 600°C, 1 h, 4A passes @ 24°C, 0 ksi
- 2B passes @ 24°C, anneal 600°C, 1 h, 4B passes @ 24°C, 5.6 ksi

The intermediate annealing treatment was performed to eliminate Zn segregation that developed during casting of the as-received materials. Previously, it was found that heat treatment of ECAE-processed brass at 600°C for 1 h was sufficient to eliminate Zn segregation. Tensile bars were made and tested. However, characterization of the

microstructure (grain size and twin grain-boundary fraction) remains before analysis of the data can be completed.

Finally, during FY 2003 a subcontract with Dr. David Field at Washington State University was placed to study the behavior of twin grain boundaries during deformation. As mentioned above, it appears twin grain boundaries act as dislocation sources during deformation. However, this has been a matter of debate for a number of years. Dr. Field was given the task to obtain direct evidence of twin grain boundaries acting as dislocation sources. Dr. Field used orientation imaging microscopy (OIM) to track the misorientation across twin related grain boundaries during deformation of annealed, ECAE-processed copper. Twin grain boundaries acting as dislocation sources will cause the orientation relationship of twin related grains to deviate from the ideal 60° rotation about the <111> direction. Dr. Field did observe the growth and disappearance of some twin related grains. Furthermore he documented a change in misorientation across the twin boundary as deformation proceeded. The results and conclusions of his study are being written up and submitted to a peer-reviewed journal for publication.

Conclusions

The work performed during FY 2003 yielded some promising results and potential uses of ECAE. Generally, it was found that ECAE processing at temperatures as low as possible produced material with the most desirable properties. An applied back stress on the sample during ECAE processing enabled the processing temperature to be reduced. Specifically, ECAE processing was used to refine the microstructure of two magnesium alloys and obtain high ductility (>200%) at moderate temperatures (200°C). Further optimization of the ECAE-processing schedule should allow superplastic forming of these alloys at relatively low temperatures (~200°C) and fairly high strain rates (10²/s or greater). High strain-rate forming capabilities will allow these lightweight magnesium alloys to be

more economically competitive (high production rate coupled with minimal scrap) with other traditional structural materials such as steel.

ECAE processing was also found to be effective for breaking up grain boundary phases and redistributing second phases. The extent of the effect is governed by the ECAE-processing temperature which controls the strength of the matrix. Hard particles in soft matrix are simply "pushed around" during ECAE processing. Stronger matrices generally afford the break up and redistribution of second phases. Again, lower ECAE processing temperatures are most desirable.

The redistribution of second phases during ECAE was found to be extremely beneficial in an aluminum alloy metal matrix composite (AL6061 + 10 wt % B₄C). ECAE processing at relatively low temperatures (~150°C) effectively breaks up agglomerates of boron carbide particles in the as-received material. As a consequence, the ductility of the composite was greatly enhanced; that is, <1% in the as-received material to around 12% in the ECAE-processed material. ECAE processing of this composite produced a lightweight material with relatively high stiffness (~78,600 MPa) for an aluminum alloy. Optimization of

the ECAE-processing parameters is expected to further increase the mechanical properties of this alloy as well as other lightweight titanium alloy composites.

Overall the main conclusion reached during FY 2003 was that mechanical properties received the most benefit when ECAE processing was carried out at the lowest possible temperature. Low ECAE-processing temperature (without sample failure) could only be achieved through the application of a back stress on the sample during processing. This result has and will allow us to ECAE process a wide variety of material with limited ductility. Materials of limited ductility are commonly found in commercial applications and therefore, ECAE processing of these materials is most relevant.

References

H. Wantanabe, et al., "Low-temperature Superplasticity of a Fine-Grained 2K60 Magnesium Alloy Processed by Equal-Channel-Angular Extrusion," *Scripta Mat.*, **46**, 2002, pp. 851–856.

E. Lightweight High-Strength Steel Alloy Castings for Heavy Vehicle Applications

Principal Investigators: Alan D. Hartman

Albany Research Center

1450 Queen Ave. SW, Albany, OR 97321

(541) 967-5862; fax: (541) 967-5958; e-mail: hartman@alrc.doe.gov

W. L. (Bill) Roberts

PACCAR Technical Center

12479 Farm to Market Road, Mount Vernon, WA 98273

(360) 757-5286; fax: (360) 757-5370; e-mail: broberts@paccar.com

Field Project Manager: Mark T. Smith

Pacific Northwest National Laboratory

902 Battelle Boulevard, Richland, WA 99352

(509) 376-2847; fax: (509) 376-6034; e-mail: mark.smith@pnl.gov

Technology Development Area Specialist: Sidney Diamond

(202) 586-8032; fax: (202) 586-1600; e-mail: sid.diamond@ee.doe.gov

Field Technical Manager: Philip S. Sklad

(865) 574-5069; fax: (865) 576-4963; e-mail: skladps@ornl.gov

Contractor: Pacific Northwest National Laboratory

Contract No.: DE-AC06-76RL01830

Contractor: Albany Research Center

Contract No.: 4400000176

Objective

- Develop and demonstrate the unique thin-wall evaporative pattern casting (EPC) technology, also known as lost foam casting, for a selected heavy vehicle chassis or drivetrain component. The project will focus on component design, castability, and performance for the selected vehicle application.

Approach

- Optimize the selected chassis component design.
- Investment-cast the designed component.
- Qualify design by dynamic testing of castings.
- Cast handmade evaporative patterns of component.
- Map the casting chemistry, especially carbon.
- Pursue permanent mold and single-piece evaporative patterns once the casting chemistry is satisfied.
- Cast commercially provided one-piece evaporative patterns.

- Evaluate castings through dynamic testing.
- Transfer thin-wall evaporative steel casting technology.

Accomplishments

- Optimized chassis design using finite element modeling and produced a stereolithographic prototype.
- Cut the stereolithographic prototype in half to facilitate investment molding.
- Produced thin-wall steel investment castings and supplied them to PACCAR.
- Completed dynamic testing resulting in an increase in fatigue life of up to four times over the life of the component currently in commercial use.
- Produced handmade evaporative patterns for proof-of-concept casting trials.
- Made EPCs with four different steel alloys for chemistry mapping.
- Procured a permanent mold for evaporative patterns after chemistry analysis showed that carbon levels could be tolerated with this application and that thin-wall casting is viable.
- Proved that commercially produced one-piece evaporative patterns are beneficial to both the resultant casting carbon chemistry and relative ease of casting with steel.
- Produced steel castings with select thin-wall areas of approximately 0.100 in. thickness by the EPC (lost foam) technology and supplied them to PACCAR for final dynamic testing.

Future Direction

- Evaluate dynamic testing results.
- Transfer the lost foam thin-wall steel casting technology to the commercial sector for this component.
- Evaluate other heavy vehicle components for potential lost foam casting applicability.

Introduction

The Northwest Alliance for Transportation Technologies (NATT) held a forum in late October 1998 with representatives from auto and truck manufacturers, light materials producers, national laboratories, and northwestern universities, among others. The forum provided the opportunity to define research needs and develop contacts for potential cooperative work. Subsequent interactions between the Albany Research Center (ARC) and PACCAR (a heavy-duty Class 8 truck manufacturer) identified areas of research that were appropriate under the NATT program.

Currently, certain aluminum cast components on heavy truck chassis must have thick cross sections in order to meet strength requirements. It would be desirable, not only for dimensional and weight reductions but also from a design standpoint, to replace the thick aluminum castings with thin-walled steel castings. [Although the term "thin-wall" is relative, it is a goal of this project to reduce wall thicknesses in sand-cast steel castings from an industry minimum of about 0.250 inches to 0.080 inches (2 mm)]. Thin-walled steel castings have a potential to increase the strength of a component while maintaining or possibly reducing the weight of an aluminum counterpart.

The EPC process will be used, and the process has demonstrated that thin-section castings can be produced. Pattern draft is minimal, dimensional tolerance and surface finishes approach investment casting quality, and EPC economies are documented, at least in the casting of aluminum.¹⁻³ The process though, has not been widely used to manufacture steel castings.

In the EPC process, molten metal is poured directly into a polystyrene pattern that is embedded in unbonded sand. The pattern vaporizes, and the metal assumes the pattern's configuration.⁴ Each casting requires a new pattern. A partial list of advantages of EPC includes

- elimination of cores
- the option of gluing simple pattern parts together to make a more complex whole
- elimination of sand binders and sand preparation equipment
- reduction of pattern and part draft
- elimination of parting lines
- reduction of post-casting cleaning
- the freedom to orient patterns in molds in a variety of positions to increase options for casting feeding and directional solidification

Although most problems in casting aluminum using the EPC process have been resolved, the techniques for aluminum EPC are not entirely transferable to steel, and additional problems have been encountered. The replacement of a pattern by molten aluminum during pouring is slow, and the pattern and aluminum are in constant contact with one another.⁵ When steel is used, however, the pattern tends to evaporate as soon as the hot metal enters the mold.⁶ Molds may collapse well before enough metal is available to replace the pattern. Steel castings may be larger than aluminum castings and consequently less rigid. Pattern handling is more difficult, especially if parts have thin walls or rangy

sections. Unique casting defects are likely if pattern byproducts are not eliminated before the liquid steel replaces the pattern.

ARC has successfully cast .125-in.-thick, slotted P-900 armor⁷ by modifying the EPC process for aluminum casting and adapting it to steel. ARC added three innovations to the EPC process for aluminum to make the adaptation successful:

- Double-walled sand flasks were developed for the application of vacuum to sand molds.
- Continuous narrow-neck feeding systems were used to deliver metal to all casting sections and permit the casting of thin walls.
- Fixtures were designed to prevent pattern damage and to hold critical casting tolerances.

The following steps briefly describe the modified EPC process for steel.

- EPC patterns are constructed by expanding polystyrene beads with pentane (thus eliminating chlorinated fluorocarbons).⁸
- Proper gating and runners are incorporated with the pattern.
- If necessary, to limit distortion, fixtures also are prepared to maintain desired casting contours. The reusable fixtures are easily inserted within a flask along with a pattern. The patterns can be flexed to the fixture contour and attached with string.
- The pattern and fixture are dipped in a slurry of fine silica and binder. Coatings help maintain the integrity of the cavity that results after the pattern evaporates upon pouring and provide a better surface finish.
- The coating is dried, and the pattern is inserted into a vacuum flask. The flask is then filled with unbonded silica sand and vibrated for compaction to make a mold.

The application of vacuum to the mold provides additional flow enhancement to ensure complete pattern filling by effectively increasing the pouring height equivalent to about 1.5 m. The vacuum also collects gases for disposal, adds rigidity to the mold, and prevents cavity collapse. Double-walled molding flasks, the inner walls of which are screened, are used to apply the vacuum. Large-diameter hoses connect the flask with a vacuum system containing a large surge tank. Systems without the surge tank appear to lack sufficient capacity to absorb the surge of gases that are generated when the pattern evaporates. The open top of the flask is sealed with plastic, and the flask is evacuated. A sand pouring basin is placed on the top of the plastic with its opening adjacent to the sprue.

After pouring, the casting is allowed to solidify and cool before removal from the flask. The spent, unbonded sand requires little post-treatment other than cooling before recycling. Casting surfaces are relatively clean, compared with castings made with other processes, because of the absence of sand binders and binder-related defects. The gates can be detached by impact with a hammer. Portions of gating that remain on the casting, although nearly insignificant, can be removed by grinding. The castings can be heat-treated using normal quench and temper cycles.

Casting Component Design

PACCAR identified components for weight reduction or conversion from aluminum. PACCAR performed finite element stress analysis to optimize the distribution of metal without regard to castability, solidification, or any other manufacturing constraints; that is, the component represented an ideal configuration from the perspective of function on a heavy-duty truck.

Therefore, three main questions needed to be researched:

1. Can an optimized component using engineered advantages, such as thin-wall sections, replace existing components at the same or reduced weight while increasing performance?
2. Can the component be cast in steel by the lost foam process and meet specifications?
3. Can a permanent mold be produced incorporating thin- and thick-walled sections to provide a one-piece foam part that can be cast in steel?

To answer question number one, PACCAR provided a stereolithographic prototype created from finite element modeling. This prototype was then used to create an investment mold. Investment steel castings were produced for proof-of-concept testing of the optimized design.

PACCAR expended considerable effort to develop and construct a testing fixture that simulated over-the-road conditions for dynamic fatigue testing of the castings. The castings were tested and proved to last up to four times longer than the current aluminum component. The added benefit was that the steel cast part was equivalent in weight. Therefore, EPC of the component was investigated next.

Evaporative Pattern Casting

The positive outcome of the design allowed us to pursue the question of using EPC. The challenges of lost foam casting with steel included pattern filling in thin-wall sections and carbon pickup being detrimental to performance specifications. Handmade 1.2 lb/ft³ polystyrene patterns were used for initial testing. The multi-piece patterns were cut, glued at the assembly joints, waxed for casting, and dried.

The pattern was then coated with a ceramic material for protection and surface finish considerations. The dried pattern was next set into a double-walled vacuum flask and buried with loose sand (Figure 1). The



Figure 1. A double wall vacuum flask is being loaded with sand around an embedded foam part for casting.

flask was vibrated to compact the sand around the pattern, and the sprue was cut off flush with the top of the flask. A plastic covering was positioned over the sand and sprue top, after which a pouring basin was placed above the sprue before a vacuum was pulled on the flask.

Designed experiments were used to determine the effects, importance, and range of such variables as pouring temperature, vacuum level, sand permeability, sand type and size, and pattern coating. The casting campaign set out to include four different steel alloys cast in triplicate. Casting conditions included a pour temperature of around 3050°F (Figure 2). The patterns were typically cast with 30 in. Hg vacuum, and shakeout occurred 1.5 hours later. Heat treatment included a 45-minute normalized cycle at 1600°F followed by air cooling and then tempering for 45 minutes at 1200°F followed by air cooling.

In general, these observations were made from the handmade foam pattern castings:

- Target melt chemistry was achieved.
- Horizontal pattern filling symmetrically distributed carbon regardless of the alloy.
- Elevated carbon levels were found in the thin sections and in the last areas to fill, with typical carbon increases of approximately 0.45 points.



Figure 2. Molten steel is being poured into a pouring basin feeding a foam pattern within the vacuum flask.

The success in filling thin sections, along with encouraging carbon pickup levels, showed the feasibility of lost foam casting for this application. Therefore, the decision was made to pursue a permanent mold for the production of one-piece foam patterns.

Permanent Mold

A major challenge presented itself in locating a mold vendor willing to take the risk of producing a mold with very thin wall (~ 0.100 in.) sections in conjunction with thick sections (~0.610 in.). Tempo Plastic Company took the challenge and delivered one-piece foam patterns for casting trials. The one-piece patterns eliminated numerous glue joints that were required in the handmade patterns. However, another variable was added in that the foam pattern density increased to approximately 3.0 lb/ft³.

The increased foam density did not adversely affect the castability of the pattern or the carbon pickup for steel. In fact, the one-piece foam pattern actually had lower carbon pickup values (approximately a 0.32 point increase) than the handmade patterns. This lower value was attributed to the elimination of the glue and wax joints.

Significant casting results included these:

- Excellent casting surface finish
- Low carbon pickup

- Use of a lower vacuum (12 in. Hg)
- Casting reproducibility

The resulting steel castings were sent to PACCAR for dynamic fatigue testing.

Conclusions

An optimized heavy vehicle component incorporating thin (~0.100 in.) and thick (~0.610 in.) wall sections was designed without regard to castability, solidification, or any other manufacturing constraints. The research has shown that this designed component can be produced out of polystyrene foam and successfully cast using the lost foam casting technique with steel. Dynamic fatigue testing remains to be completed. Results up to this point offer encouragement that the lost foam casting technique can be adapted to steel, making it possible to cast complex structures and thin-wall components.

References

1. P. G. Kohler, "Evaporative Pattern Process: A New Dimension for the Foundry," *Modern Casting*, August 1981, 36–37.

2. E. Wessman and R. Mrdjenovich, "Update: ECP Goes On Line at Ford's Essex Plant," *Modern Casting*, March 1985, 30–31.

3. E. F. Longnecker, K. Kanoh, and J. S. Fukuya, "Pioneering Evaporative Foam Iron Casting Production in Japan," *AFS Trans.*, 96, 89–94 (1988).

4. R. Bailey, "Understanding the Evaporative Pattern Casting Process (EPC)," *Modern Casting*, April 1982, 58–61.

5. S. Shivkumar, L. Wang, and D. Apelian, "The Lost-Foam Casting of Aluminum Alloy Components," *Journal of Metals*, November 1990, 38–44.

6. Y. A. Stepanov and D. S. Grishin, "Casting Steel in Moulds With Gasifiable Patterns," *Russ. Cast. Prod.*, (Birmingham, Eng.), 1972, 189–192.

7. J. S. Hansen, and P. C. Turner, "Casting P-900 Armorplate by the Expendable Pattern Casting Process," *Report of Investigations 9436*, U.S. Bureau of Mines, 1992, 1–7.

8. R. H. Immel, "Expandable Polystyrene and Its Processing into Patterns For the Evaporative Casting Process," *AFS Trans.*, 87, 1979, 545–550.

F. Development of an Advanced Squeeze Casting Process for the Production of High-Integrity Truck Components

Principal Investigator: David C. Weiss

Eck Industries, Incorporated

1602 North 8th Street, Manitowoc, WI 54221-0967

(920) 682-4618; fax: (920) 682-9298; e-mail: dweiss@eckindustries.com

Technology Development Area Specialist: Sidney Diamond

(202) 586-8032; fax: (202) 586-1600; e-mail: sid.diamond@ee.doe.gov

Field Technical Manager: Philip S. Sklad

(865) 574-5069; fax: (865) 576-4963; e-mail: sklads@ornl.gov

Contractor: Eck Industries, Incorporated

Contract No.: 4000022893

Objective

- Develop the equipment and process technology for an advanced squeeze casting (ASC) process to enable production of high-integrity cast metal components.
 - Integrate the advantages of two casting methods—low-pressure permanent mold and direct squeeze casting—to attain (1) nonturbulent fill of the die, (2) high solidification rates to refine microstructural features, and (3) solidification under pressure to minimize microporosity.
 - Design and build a new kind of casting machine and develop process technologies needed to cast high-integrity truck components from nonferrous alloys.

Approach

- Design and construct a casting machine that integrates a low-pressure metal delivery system suitable for either aluminum or magnesium, reliable gate shut-off technology, and direct application of squeeze pressures up to 103 MPa (15,000 psi). This machine is intended for production.
- Develop a gate shut-off mechanism that will operate reliably in a production environment.
- Select a casting that will be produced in the casting machine built for this project.
- Use fluid-flow and solidification analysis to predict optimum flow conditions for metal entering the mold and differential squeeze requirements.
- Design and build cast tooling.
- Develop process technologies for the low-pressure/squeeze casting of aluminum alloys and evaluate the effect of various process parameters on casting integrity.
- Apply development results to the production of a selected automotive component.

Accomplishments

- Completed preliminary design of the casting machine.
- Designed experiments for development of reliable gate shut-off mechanism.

- Selected a connecting rod for a Bendix truck air compressor as a production part.
- Acquired software for die fill and solidification analysis.
- Completed the preliminary design of cast tooling.

Future Direction

- Complete design of casting machine.
- Complete design of gate shut-off mechanism, and integrate this mechanism with the casting machine control system.
- Fabricate casting machine and install at Eck Industries.
- Complete cast tooling design and fabricate.
- Develop and evaluate ASC process technologies.
- Demonstrate production viability of ASC casting machine and process.

Introduction

Squeeze casting is the solidification of liquid metal under pressure in a closed die. The resultant casting has improved properties and created a more uniform microstructure as compared to those produced by traditional molten metal fabrication techniques. The improved properties are achieved through controlled entry of the metal into the die through large gates. This entry reduces turbulence and high solidification rates, resulting in the refinement of microstructural features.

The method and efficiency of pressure application distinguish the two types of squeeze casting (direct and indirect). Direct squeeze casting is the most efficient (essentially 100%) as it applies pressure directly on the casting. This contrasts with indirect squeeze casting in which pressure is applied using the gating system. The length of the gating system and any partial solidification caused by the gating system prior to complete solidification of the part reduces the pressure applied to the part and results in casting porosity. For the indirect squeeze cast method the dimensions of the die cavity control part dimensions. For the direct squeeze cast method, the part dimensions are controlled by the die cavity dimensions and the finish position of the

top die. Thus, the direct squeeze cast method requires precise machine control to attain the desired part dimensions. The hot metal handling technique for transporting the metal from the furnace into the mold or gating system is deficient for both the direct and the indirect squeeze cast methods. The current method introduces additional casting defects such as oxide inclusions that are especially detrimental, causing increased fatigue properties.

Earlier attempts to improve the squeeze casting process by combining the advantages of low-pressure die fill with those of squeeze casting demonstrated the ability to produce high-integrity components; however, continuous production operation of the equipment was not achieved. The machines used were not specifically designed to meet the needs of the process.

Technical Approach

This recently initiated (June 2003) project will (1) design and develop a production-viable ASC machine, (2) develop process technology that will improve the strength and reliability of cast automotive components, and (3) demonstrate the production viability of the equipment and process.

An assessment of the capabilities and limitations of existing cast machine designs demonstrated that

- Low-pressure casting machines typically do not have the structural rigidity to resist the high pressures applied during the squeeze casting process.
- Die-cast and squeeze-cast machines are not designed to accommodate nonturbulent molten metal entry into the die cavity.
- Neither type of equipment is typically set up with the type of hydraulic and electronic controls necessary for the cavity movement envisioned as required for the ASC process.

Therefore, the project team decided to design and build a machine from the “ground up” instead of modifying an existing low-pressure, die-cast or squeeze-cast machine. The project team partnered with Empire Castings, Inc., an experienced producer of low-pressure casting equipment, to design and construct the ASC machine.

Through consultation with Bendix, Inc., an industrial manufacturer of truck components, a casting(s) will be chosen for production in the ASC machine. The selected component will meet the following criteria:

- A level of complexity that can demonstrate the production capability of the ASC machine.
- A requirement for mechanical properties higher than those attainable with commercially available castings.
- An opportunity for the casting selected or one similar to it to move into production with the ASC process.

The casting selected, an air compressor connecting rod, will be modeled for fluid flow and solidification shrinkage. This work will be done in parallel with equipment design. This model should enable us to understand optimum flow conditions for metal entering the mold and differential squeeze requirements, if any, to contend with solidification shrinkage. Modeling of

the casting is very important to the success of the program and, potentially, to the details of the machine design. The ASC machine has two mechanisms to feed the casting—low-pressure, nonturbulent fill of the die cavity and high-pressure, direct squeeze to minimize solidification shrinkage. Modeling experiments will explore the interaction of the two feed mechanisms and select process parameters that lead to process optimization. Modeling results will be used to refine the die design and select initial casting process parameters.

After tooling construction and ASC machine delivery, castings will be operated under a range of process conditions anticipated during modeling, using a variety of cast and wrought alloys (Table 1). Analysis of those castings will include radiography, die penetrant inspection, tensile testing, and functional component testing at Bendix. It is anticipated that this part of the program will involve multiple iterations in order to produce the product successfully. Some equipment and tooling modification may be required during this part of the program.

Table 1. Aluminum alloys to be used for casting trials

AA 380	AA 206
AA 356	AA 6061
AA 357	AA 535
AA 319	AA 388

After successful production of development castings, the production viability of the equipment and process will be demonstrated. This will be done by

- Production of a connecting rod with reduced porosity and improved mechanical properties as compared to the current die-cast connecting rod used by Bendix.
- Continuous production of the ASC machine and connecting rod tooling to include at least one 5-h continuous run with the equipment running at least three days in a week.

It is the goal of the project team to implement part production on an ongoing

basis. The production phase of the project will include detailed cost analysis of part production, determination of die-life parameters, and ongoing equipment and tooling development for maximum uptime.

Program Schedule

The scheduled start and end dates for the various program tasks are listed in Table 2.

Table 2. Overall program schedule

	Start date	Completion date
Machine design	June 2003	Nov. 2003
Machine build	Nov. 2003	Mar. 2004
Tooling design	July 2003	Oct. 2003
Tooling build	Nov. 2003	Mar. 2004
Process modeling	Oct. 2003	Dec. 2003
In-gate S.O. development	Nov. 2003	Dec. 2003
Machine install	Mar. 2004	Apr. 2004
Casting development	Apr. 2004	June 2004
Evaluation and testing	May 2004	Oct. 2004
Final report	Apr. 2004	Dec. 2004

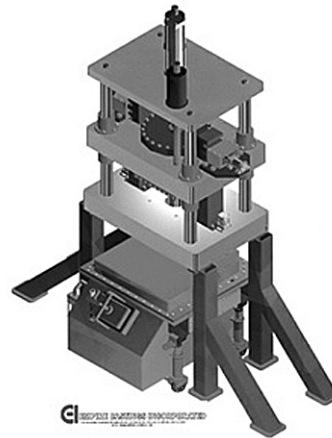


Figure 1. Overall design concept for 600-ton ASC machine.

To match the dimensional capabilities of the die-cast process, a closely controlled volume of liquid metal must be fed into the die cavity. Conventional low-pressure fill technology does not have the capability to accurately meter a fixed amount of liquid metal into the die. Therefore, we will accurately position (± 0.05 mm) the top die to obtain the desired fill volume and use a fill sensor and an independently controlled gate shut-off to control metal volume. Development of a reliable gate shut-off technology is a key part of the experimental program.

Machine Design Status

Initial design (Figure 1) of the 600-ton capacity ASC machine has been completed. Positioning of the top die is accomplished independently of the squeeze-cast cylinder. To maximize machine capability, the melting vessel will be equipped with a crucible furnace. This will facilitate the melting of cast and wrought aluminum and magnesium alloys as well as aluminum and magnesium metal matrix composite alloys.

Tooling Design Status

The die for the ASC machine consists of a die holder and individual die inserts for the particular part being cast. The die casting tool is shown in Figure 2. The location of the inserts for a test bar blank and an air compressor connecting rod is shown in Figure 3. The size and configuration of the gating will be finalized when the fill and solidification modeling is complete.

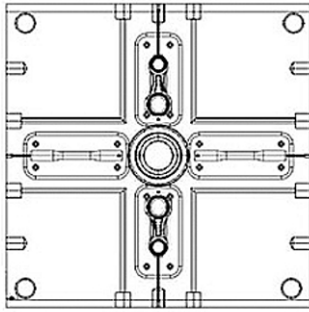


Figure 2. View of cast tooling.

Conclusions

Excellent progress has been made on design of a production ASC machine and the cast tooling for development of casting process parameters. All tasks are currently on schedule for completion of the program within the time allotted.

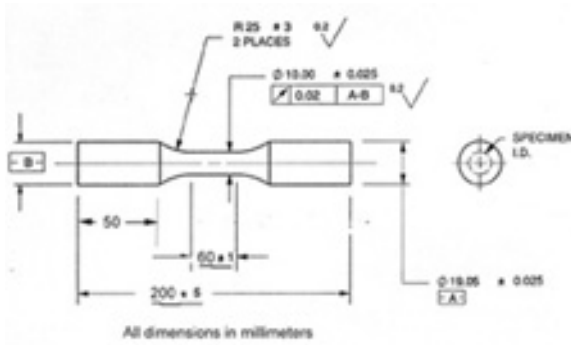


Figure 3. Cast tensile test bar configuration.

G.Ultra-Large Casting Benchmark Study for Aluminum and Magnesium Alloys: Phase II

Principal Investigator: Thomas N. Meyer, Ph.D.

Consultant

3987 Murry Highlands Circle, Murrysville, PA 15668

724-325-2049; fax: 724-325-9159; e-mail: tnmeng@aol.com

Technology Development Area Specialist: Sidney Diamond

(202) 586-8032; fax: (202) 586-1600; e-mail: sid.diamond@ee.doe.gov

Field Technical Manager: Philip S. Sklad

(865) 574-5069; fax: (865) 576-4963; e-mail: skladps@ornl.gov

Contractor: American Foundry Society, Des Plaines, IL 60016

Contract No.: 4000012401

Objective

- Evaluate candidate casting processes for producing magnesium or aluminum alloy lightweight ultra-large thin-wall structural castings for automobiles and light trucks.
- Compare the energy required to produce a minivan inner panel based upon (1) a conventional manufactured assembly of steel stampings and (2) a lighter-weight aluminum casting of the same part.

Approach

- Assess five metal casting processing routes:
 - Multi-port hot chamber injection at pressures compatible with permanent mold systems
 - Single gas plenum driving metal to fill a permanent mold
 - A combination of pressurized gas and vacuum metal filling for producing both magnesium and aluminum permanent mold castings
 - A low-cost semi-solid process to produce aluminum castings
 - A process requiring magnesium chips to produce a cast magnesium component in a semi-solid process
- Determine the energy required to produce an aluminum liftgate inner panel casting for a minivan and the energy required to produce the same component based upon an assembly of steel stampings as is currently practiced
- Recommend steps toward achieving lightweight vehicle structures at costs competitive with those of current structures.

Accomplishments

- Developed a test part configuration for evaluating candidate process capabilities that embodies key casting geometric features typical for ultra-large structural castings: thin/thick/thin

transitions, representative distance between metal entry and knit lines, flow distances, and geometry characteristic of structural components.

- Identified an opportunity to evaluate a large “body on frame” structural part of specific interest to an original equipment manufacturer (OEM) using the Thixomat process (i.e., process 5 under “Approach”) and outlined the project tasks, schedule, and conceptual budget.
- Conducted an energy analysis, principally at Oak Ridge National Laboratory (ORNL), that clearly indicates that employing aluminum structural castings saves energy.

Future Direction

- Develop a detailed design of a test part for evaluation of the candidate processes that
 - includes the representative geometry of vehicle structural parts
 - minimizes the cost of tooling
- Fabricate tooling for the test part so that it is compatible with equipment for the different processes of interest (e.g., vacuum die casting, semi-solid aluminum and magnesium processes, and permanent mold processes).
- Using the same test part tool set, evaluate processes in a prioritized order.
- Initiate demonstrations of the semi-solid magnesium process to produce a large body on frame part (i.e., 1.1 m²) for OEM application through the U.S. Automotive Materials Partnership (USAMP).
- Direct efforts toward development of a reliable molten metal injector system. This will require materials development for key areas of the molten metal pump.

Introduction

The ability to produce aluminum or magnesium ultra-large thin-wall structural castings (ULCs) is key to lightweighting auto and truck structures at costs competitive with those of heavier steel assemblies. Castings offer the potential for both cost and weight reduction compared with sheet components. The definition of a ULC is subject to judgment, but the following specifics are offered to better define ULCs as discussed in this study:

- The part area is greater than 1 m² (e.g., typical of a minivan liftgate inner).
- As a result of a combination of weight and stiffness requirements, wall thickness will range between 2 and 3 mm for much of the part area.
- Bosses and attachment areas will be much thicker (e.g., 6 to 8 mm).

- The minimum major dimension is 120 cm.
- The minimum minor dimension is 90 cm.

ULC offer a cost advantage due to reduction in the part count (e.g., 10×) and assembly of stampings to produce the final component. Examples include an auto sidewall aperture structure or a vehicle floorpan frame. This approach also simplifies the supply chain and decreases the time to market. High-strength steels may be used to save weight but only at a cost premium, using established supply chains. As was learned from Ford’s conversion of the F-150 radiator support structure from an assembly of steel stampings to a magnesium casting, additional weight can be saved because of system considerations that go beyond simple component substitution. However, sheet components (e.g., steel, aluminum) will be

required for exterior components because castings currently cannot provide the Class A finish required for the vehicle exterior surface.

ULCs offer weight reduction that translates into reduced vehicle fuel consumption and reduced emissions. Such energy and environmental considerations are the primary drivers for lightweighting vehicles. However, a demonstrated advancement in casting technology will benefit other industries that can employ castings. For example, the aircraft industry has been under increasing pressure to reduce manufacturing costs. Heavy ground vehicles such as buses and trucks also will make greater use of lightweight castings.

Many of these opportunities are directed to products that have volumes of less than 50,000 units or even less than 1,000 units per year. Because of high tooling costs for the fabrication and assembly of sheet-formed components, manufacturing costs can be very high at these low volumes. For example, the tooling cost for an inner liftgate panel is \$6.5 million. Currently, the heavier steel sheet-formed components are more cost-effective at volumes in the range of 100,000 to 400,000 units. Even for such high volumes, it is anticipated that structural components comprising many individual stampings will not remain cost-competitive versus a single lightweight casting beyond the next 10 to 20 years. Castings will continue to displace assemblies of stamped components.

It is implicit that the newly developed technologies concomitantly at least maintain current safety performance and possibly enhance safety. Structural parts must possess a ductility exceeding 8%, although some specific areas may not require this level of ductility.

Scope

This second-phase casting benchmark study is directed to evaluating processes considered best for producing ULCs of

magnesium or aluminum alloys. The first phase, completed in July 2002, identified five casting processes potentially capable of achieving this goal. A cost analysis indicated that these processes are capable of producing ULC components at costs competitive with those of conventional assemblies of steel stampings. Although steel stampings are cost-effective at high production volumes, ULCs are cost competitive from very low volumes to as much as 70,000 units per year. Because of tooling costs, the permanent mold processes provide the lowest-cost ULCs.

Although Phase I identified candidate casting processes for producing ULCs, more information was needed prior to proposing specific demonstration and evaluation projects. Five process routes were assessed:

- Multi-port hot chamber injection at pressures compatible with those of permanent mold systems
- Single gas plenum driving metal to fill a permanent mold
- A combination of pressurized gas and vacuum metal filling (like the Brocast process developed in France)
- A semi-solid process for producing aluminum castings having T5 properties exceeding typical T6 properties
- A semi-solid magnesium process that does not require handling of molten magnesium

A Sixth Alternative

The conventional vacuum die casting process, as practiced at Alcoa, Gibbs, and other foundry operations, was also considered for ULC. Presses and dies may be built with sufficient tonnage (i.e., 10,000 to 20,000 tons). However, the cost of parts, particularly at low volume, may still be an issue because of higher die costs relative to the costs of three low-pressure processes described earlier. For example, vacuum die casting part costs are projected to be 20 to 30% higher than the cost of parts produced by the permanent mold process at volumes

in the range of 15,000 to 30,000 units per year. However, cost reductions for die castings are expected to continue, and vacuum die casting cannot be eliminated as an approach to ULCs.

All of these processes have the potential to produce ULCs at costs competitive with the cost of stamped steel assemblies at various production volumes (i.e., crossover points) established by specific manufacturing considerations. Generally, at still lower volumes, casting becomes the low-cost choice while saving weight.

Permanent Mold Process Alternatives

The first three ULC process alternatives are permanent mold processes.

Multi-port hot chamber injection

Multi-port hot chamber injection at pressures compatible with those of permanent mold systems is an extension of the route pursued by Alcoa from 1996 through 1999. Significant development of the hot chamber injection system is required before the process can realize a low-cost production capability. Unlike in gas pressurization, the metal injection can be controlled precisely. However, significant development of the injector components is required.

Pressurized gas filling

Several factors could limit the size of parts produced with low-pressure gas driven processes (2 and 3). Larger castings require the use of hot runner systems employing heavy mold coatings and tighter temperature control. Such control can be extremely difficult. A second alternative uses multiple feeds, requiring a large pressurized molten metal furnace or a distribution box nearly equivalent in size to the part plan area. A large high-temperature vessel subject to cyclic pressurization can be a real challenge as furnace sizes increase.

The pressurization process that resembles the Brocast process requires similar considerations. During the cycle, pressures can be controlled from 0.05 atm absolute to as high as 15 atm. Using this process in the future for production of full-scale ULCs will require

- manufacture of a metal holding vessel with appropriate fill point locations permanently fabricated in the pressure vessel;
- employing a heated Bosch (i.e., manifold for molten metal) for metal distribution to the mold fill point locations; or
- using multiple smaller metal containers or pressure vessels, provided the spacing between metal entry to the mold is not too close.

Three major challenges are (1) these modifications are significant steps over current capability, (2) tooling technology for such high vacuums does not exist at Brocast, and (3) the intellectual property resides off-shore.

High-Pressure Injection Process Alternatives

The last two processes are more similar to the sixth alternative, die casting (i.e., relatively high-pressure injection). The first is a semi-solid casting process to produce aluminum castings. The properties of castings produced in this process in the as-cast condition (T5 temper) are comparable to castings that are solution-treated and aged (T6 temper). With the elimination of high-temperature heat treatments for ULC parts, dimensional management is significantly eased. In addition, the tooling and caster capital costs are significantly lower than those of vacuum die casting. The maximum casting pressure is 8000 psi, which is 40% below that of some die casting pressures. However, there is uncertainty whether the process can flow metal over distances necessary for ULC parts.

The second process (like the Thixomat process) converts a feedstock of chips (not molten metal) to a semi-solid state and injects them in a process similar to what is used in die casting. Although comparable equipment is not available for aluminum, the process is expected to be compatible with multiple injectors. The commercial application of the Thixomat magnesium casting process has grown rapidly for small thin-wall parts typically found in portable communication, computing, and video equipment. The same process is now aggressively targeting larger automotive parts, and some automotive parts are currently in production. Because it avoids the handling of molten magnesium alloy and provides a high yield, the process is extremely attractive. ULC capability will depend upon major developments under way to perfect hot runners and inductively heat the feed material in the injector barrel.

Current Status

At present, none of the processes is ready to produce ULCs. One might argue that vacuum die casting is the closest to meeting ULC requirements. However, equipment becoming available by April 2004 will enable demonstration of ULC production. Such a demonstration will be based upon a test part design that simulates key features of a ULC without requiring either a large machine or a complex and expensive mold tooling. (Such a test part is described in the final report available through the American Foundry Society.¹) This can be readily done for all the processes discussed except the multi-port hot chamber injection process.

Tasks, schedule, and conceptual budget were prepared for such a demonstration of each of these processes and vacuum die casting. The cost to demonstrate the ULC capability with the test part is less than \$800,000, and the task can be completed in less than 16 months. If a second process is evaluated and the test part tooling is designed to be compatible, the cost of the

test part design and the tooling will be substantially lower, and the overall test cost may be less than \$450,000. Priorities must be established.

Similarly, tasks, schedule, and conceptual budget to develop a multi-port hot chamber injection system were prepared. The potential for a low-cost product produced by this process is enormous. The pursuit of multi-port hot chamber injection is considerably more expensive (\$2.2 million) and will require as much as 2 years for a similar ULC demonstration.

Energy Comparison

A comprehensive energy analysis was conducted to compare structural parts produced in aluminum castings with those produced as a traditional stamped steel assembly. Any such analysis depends upon specific assumptions, but the study clearly indicates that the additional energy for producing the aluminum over steel is saved within the first vehicle lifetime (see Figure 1) and available for subsequent generations without and energy penalty. In a

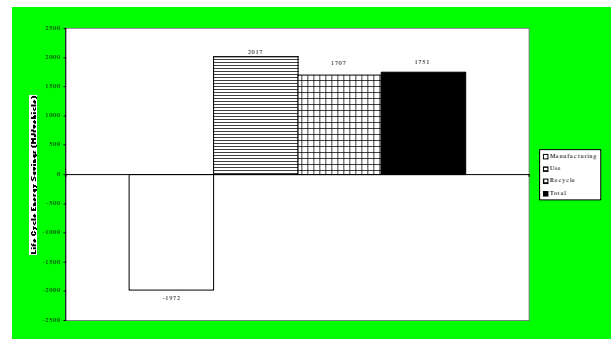


Figure 1: Life cycle energy savings of cast aluminum liftgate vs stamped-steel liftgate.

conservative case of a minivan liftgate inner panel (Figure 2) having a weight savings of 21%, the added energy to produce the aluminum is returned in the first vehicle life. However, more typical weight savings of 30% to 40% provide positive energy benefits within the first few years of vehicle life. This



Figure 2. Casting targeting Daimler-Chrysler liftgate inner.

energy savings, as well as the reduced environmental impact, strengthens both domestic energy independence and manufacturing competitiveness. High-strength-steel stamped components offer another option to save weight, but costs are greater and thus they are not attractive.

Recommendations

- Design a ULC test part and corresponding tooling such that the “test part” represents key features of a structural ULC (e.g., thin/thick/thin transitions, cross section profile, thickness, metal flow to knit-line distance).
- Minimize the cost of tooling.
- Design the tooling to be compatible with equipment for processes of interest (as much as possible).
- Using the test part tooling, begin evaluating ULC capability for each of the processes in order of priority (e.g., probably examining vacuum die casting first).
- Demonstrate production of an OEM body on frame structural component employing the Thixomat semi-solid magnesium process.
- Develop the hot chamber injectors multi-port low-pressure injection system.

- Demonstrate the hot chamber injectors can produce the test part at available commercial facility.

Pressure-driven processes are practiced globally today. Process improvements will naturally continue for high-volume gas-pressurized systems. Issues such as large pressurized furnaces, employment of hot metal manifold systems, and indirect control of metal flow lessen interest in these processes. Thus, gas-pressurized metal permanent mold casting will continue to improve with market forces, without government-shared risk in emerging technologies with new capabilities.

Demands will continue for casting capabilities to become larger and capable of more complex section geometry. This demand is driven by market forces to reduce the cost of manufacturing vehicle structures and regulatory forces for energy efficiency and environmental benefits. Working together, government agencies (e.g., DOE) and OEMS (through organizations like USAMP) will help reduce the technical risks and hasten these benefits to society. Technology conduits (e.g., the American Foundrymen’s Society) provide a fertile medium where converging private wants and public needs can be effectively integrated in specific programs to meet these goals.

This is the second phase of a benchmark study to evaluate candidate casting processes for producing magnesium or aluminum alloy lightweight ultra-large thin-wall structural castings (ULC) for autos and light trucks. These parts have projected areas exceeding 1 m². Examples include an auto sidewall aperture structure or a vehicle floorpan frame (see Figure 3). ULCs can replace the assembly of ten or more steel stampings. The first phase of the benchmark study, completed in July 2002, identified five casting processes of interest. Castings were determined to be cost-effective beginning at low volumes and continuing to volumes as high as 70,000 units per year. At the highest volumes, the

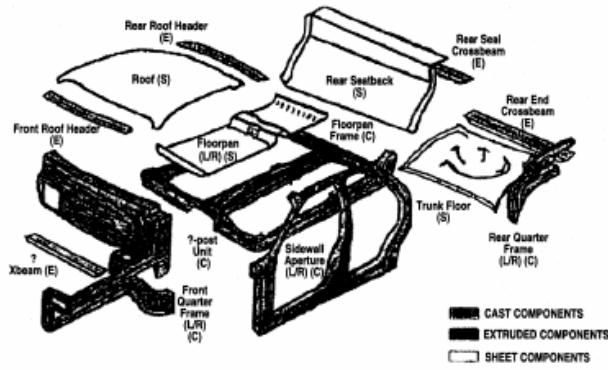


Figure 3. Candidate vehicle cast components.

process of steel stampings continues to be most cost-effective.

Although the lowest costs are projected for a multi-port hot chamber process, technical risks for this technology are judged too great at this time.

Reference

1. T. N. Meyer, *Ultra Large Casting Benchmark Study for Aluminum and Magnesium Alloys: Phase II, AFS Project ORNL-ULC-11, July 2003.*